JIMMA UNIVERSITY
POST-GRADUATE STUDIES
COLLEGE OF NATURAL SCIENCE
DEPARTMENT OF CHEMISTRY

SYNTHESIS AND CHARACTERIZATION OF NITROGEN AND PHOSPHORUS CODOPED ZINC OXIDE NANOCOMPOSITE FOR PHOTOCATALYTIC DEGRADATION OF METHYLENE BLUE, ANTIMICROBIAL AND ANTIOXIDANT ACTIVITIES

BY: ADEM ABDULKADIR

ADVISORs: TAMENE TADESSE (Ph.D)

TILAHUN YAI (MSc)

November 2023

Jimma-Oromia-Ethiopia

SYNTHESIS AND CHARACTERIZATION OF NITROGEN AND PHOSPHORUS CODOPED ZINC OXIDE NANOCOMPOSITE FOR PHOTOCATALYTIC DEGRADATION OF METHYLENE BLUE, ANTIMICROBIAL AND ANTIOXIDANT ACTIVITIES

BY: ADEM ABDULKADIR

ADVISORs: TAMENE TADESSE (Ph.D)

TILAHUN YAI (MSc)

A THESIS SUBMITTED TO JIMMA UNIVERSITY SCHOOL OF GRADUATE STUDIES COLLEGE OF NATURAL SCIENCE CHEMISTRY DEPARTMENT IN PARTIAL FULFILLMENT OF THE REQUIREMENTS FOR THE MASTER'S DEGREE OF SCIENCE IN PHYSICAL CHEMISTRY

A Thesis Submitted to Jimma University School of Graduate Studies College of Natural Science Chemistry Department in Partial Fulfillment of the Requirements for the Master's Degree of Science in Physical Chemistry

Approved By:

Advisor	Signature	Date
Tamane Tadasse (Ph.D)	_____	_____
Tilahu Yai (MSc)	_____	_____

Jimma University College Of Natural Sciences

Department Of Chemistry

Department Head	Signature	Date
Kasim Kedir (M.Sc.)	_____	_____
Examiner	_____	_____

Contents Pages

LIST OF FIGURES

LIST OF TABLES

ACKNOWLEDGEMENT

Firstly, I would like to acknowledge God who gave me strength and patience throughout the work and being with me. Then, I would like to express my deepest gratitude to my advisor Dr. TAMENE TADASSE, and Co-advisor Mr. TILAHUN YAI for their guidance, constructive comments, valuable suggestions, advice, and support without any tedious for better preparation of this research work.

Lists of Acronyms

CNS	Central Nervous System
DMSO	Dimethyl Sulfoxide
DPPH	2,2-Diphenyl-1-Picrylhydrazyl-
DW	Distilled Water
eV	Electron Volt
FT-IR	Fourier Transform Infrared
JCPDS	Joint Committee on Powder Diffraction Standards
MB	Methyl Blue
MIC	The Minimum Inhibitory Concentration
MONPs	Metal Oxide Nanoparticles
MW	Microwave
NCs	Nanocomposites
NPs	Nanoparticles
PEC	Photoelectrochemical
PZC	Point Zero Charge
ROS	Reactive Oxygen Species
RSA	Radical Scavenging Activity
SEM	Scanning Electron Microscopy
SMO	Semiconducting Metal Oxide
UV-Vis	Ultraviolet-Visible
VO	Oxygen Vacancies
Van	Zinc Vacancy
XRD	X-Rays Diffraction
Zuni	Zinc Interstitials
ZnO-NPs	Zinc Oxide Nanoparticles

ABSTRACT

Nanotechnology has wide applications in various fields such as photocatalytic degradation, medicines, antioxidants, antimicrobials, and other fields. ZnO-NPs are the most important among the Nanoscale materials background expanding growth. In comparison, pure ZnO-NPs have been announced to have a large energy band gap, electron-hole pair rearrangement, invisible light absorption, and low photocatalytic activities which decide their capability aids. The ZnO-NPs were characterized by different techniques such as X-ray diffraction (XRD), Fourier transform infrared (FTIR) spectroscopy, ultraviolet (UV) spectroscopy, and scanning electron microscopy (SEM). In addition, ZnO-NPs can be prolonged through the combination of a small quantity of codoping of Nitrogen and phosphorus to solve these problems. We obtained the photocatalytic degradation of Methyl blue (MB) dye with pure ZnO-NPs mixed with a small amount of P and N-codoped ZnO-NCs materials. As a result, P and N-codoping ZnO-NCs reduce the energy band gap from 2.92 to 2.53 eV and substantially increase their photocatalytic activity. MB was degraded (97 %) after 80 minutes when 15 mg of P and N-codoped ZnO-NCs combined with ZnO-NPs were combined. By identification, the Nanocomposie's photocatalytic activity was greater than that of pure ZnO-NPs. Stability enhancement and surface charge are answerable for the amazing photocatalytic improvement. As we know, this is the most important photocatalytic improvement accomplished by integrating a small amount of P and N-cooped ZnO-NCs into pure ZnO-NPs. Prepared NPs and NCs were examined for anti-oxidant properties using DPPH radical scavenging activity, the tendency to scavenge the DPPH radical was increased as the concentration of NPs and NCs increased result indicates that NCs can protect oxidation by transferring electron density from oxygen to carbon through $n \rightarrow \pi^*$ transition. The NCs antimicrobial activity is reparable to that of ZnO-NPs, N-doped ZnO-NPs, and P-doped ZnO-NPs indicating that combination ZnO-NPs better advance the NCs antimicrobial activity. The photocatalytic degradation effectiveness in the reusability of P and N-codoped ZnO-NCs decreases in the order of 97 %, 91 % and 87% in the first, second and third cycles respectively may be due to the aggregations of waste ions and catalyst dosage indicating impurities.

Keywords: *Sol-gel method, P and N-cooped ZnO-NCs, Photocatalytic activity, Methyl Blue, Nanocomposite, Nanoparticles, Energy band gap.*

1. INTRODUCTIONS

1.1. Background of the study

Nanotechnology has recently been thought about as the most influential solution of creative technology materials that have a measurement nanoscale of 100 nm [1–3]. The preparation of a new significance and application of achievement of a particular area in the fields of material science engineering has been used by nanotechnology fields such as electronics, optics, biomedicines, material science chemicals, agriculture, pharmaceuticals, mechanical and food processing industries [4, 5].

Metal oxide nanoparticles (MONPs) are very important Nanomaterial that can be used in different applications, such as catalysis, optoelectronic materials, sensors, and improving environmental damages [6]. Out of the most surprising common metal oxide nanoparticles (MONPs) on Nanomaterials such as NiO, TiO_2, ZnO, Fe_2O_3, CuO, CuO_2, Ag_2O, WO_3, etc. [7], have been investigated for different applications due to their varied metal to oxygen ratio, a huge number of materials introduce in stages with different structures, properties, broad optical and electrical characterizations, and particularly the solar water splitting methods to obtain a relatively a higher organization of electron productive use in photocatalysis [8].

Out of MONPs, researchers have gained significant interest in zinc oxide nanoparticles (ZnO-NPs) for their productive antimicrobial agent against pathogenic microorganisms. They are non-toxic in low concentration, environmentally biodegradable, have chemical stability, and supercilious photocatalytic properties, and are cost-effective [9]. ZnO-NPs can be extensively used for medicines, food additives, agriculture, batteries, photocatalysts, antioxidants, cosmetics, and antimicrobial agents [4, 10]. This compound readily pierces or permeates food, to expel harmful microorganisms, and prevent them from acquiring different diseases.

Additionally, it is highly amusing the photocatalytic degradations of some obstinate dyes that cause harsh or severe face environmental pollution. In whatever the way significance of UV light active material ZnO could be altered by tuning the band gap (3.37 eV) to form visible light active materials [6, 9]. It’s of great importance to modify ZnO-NPs, to optimize sunlight prevailing

practices and improve optical properties. The physical and chemical properties of ZnO-NPs could be tuned by converting their morphology using various preparations to convey and constitute different materials. Preparation of ZnO-NCs to refine the disadvantage incorporated with the bare ZnO-NPs.

So far, we have interpreted the result combination of P-doped ZnO-NPs and N-doped ZnO-NPs into ZnO-NPs and the synthesis of nanocomposite materials P and N-codoped ZnO-NCs on its energy band gap and the kinetics of the photocatalytic degradation of methylene blue dye. Correspondingly, the chemical Sol-gel method prepared ZnO-NPs and their P-doped ZnO-NPs and N-doped ZnO-NPs nanocomposites (P and N-codoped ZnO-NCs) successfully [7, 12]. The optical properties of the prepared nanoparticle and its codoped were examined by using the spectrophotometric technique (UV-Vis spectrophotometer) and found that the incorporation of P-doped ZnO-NPs and N-doped ZnO-NPs shifted the maximum absorbance wavelength towards red [13]. Succeeding the absorbance shift, the energy band gap of ZnO-NPs was also decreased from 2.92 to 2.53 eV. Due to the reduction in band gap, P-doped ZnO-NPs and N-doped ZnO-NPs combinations into ZnO-NPs displayed higher photocatalytic activity than bare ZnO-NPs in degrading methylene blue dye [14]. This study gives significant band gap reduction, super high photocatalytic performance, and excellent antimicrobial activity and antioxidant of the P and N-codoped ZnO-NCs compared with ZnO-NPs [15, 16].

1.2. Statement of the problems

Organic dyes and their wastes that are released from different components including the mining, textile, paper printing, food processing, pharmaceutical, and leather industries are serious problems. Nanotechnology illustrates extreme potential to manufacture and use new and cost-effective techniques for the discovery and observation of contaminants, and photocatalytic degradation via catalysis. Besides infectious diseases, special bacteria are the most common due to the evaluation of drug-resistant bacteria that harm human health problems worldwide. The finding and improvement of antimicrobials are the most effective accomplishments of modern science and technology for the handling of infectious diseases. Nanoparticles have been assigned a particular study of consideration as antimicrobial activity due to their nanometer size, fluorescence ability, great biocompatibility, low toxic effect on human cells, and so on. Among

those Nanoparticles ZnO-NPs, P-doped ZnO-NPs, N-doped ZnO-NPs, and P and N-codoped ZnO-NCs could solve an achievable forthcoming resolution against drug-resistant microbial.

In this research, the following questions will be answered:

- What is the effectiveness of ZnO-NPs, P-doped ZnO-NPs, N-doped ZnO-NPs, and P and N-codoped ZnO-NCs photocatalytic degradation of MB dye?
- Do synthesized ZnO-NPs, P-doped ZnO-NPs, N-doped ZnO-NPs, and P and N-codoped ZnO-NCs effective antimicrobial activity and ZnO-NPs and P and N-codoped ZnO-NCs effective antioxidant?
- What is the environmental protection, for the removal of contaminated waste water from the environment?

1.3. Objectives of the Study

1.3.1. General Objective

The general objective of this study is:-

- To investigate the impact of codoping P and N on the photocatalytic activities, antimicrobial activities, and antioxidants of ZnO-NPs.

1.3.2. Specific Objectives

The specific objectives of the study are the following

- Synthesizing ZnO-NPs, P-doped ZnO-NPs, N-doped ZnO-NPs, and P and N-codoped ZnO-NCs.
- To characterize the synthesized ZnO-NPs, P-doped ZnO-NPs, N-doped ZnO-NPs, and P and N-codoped ZnO-NCs using UV-Vis, XDR, FTIR, and SEM
- Evaluation of photocatalytic activity and antimicrobial activity of ZnO-NPs, P-doped ZnO-NPs, N-doped ZnO-NPs, and P and N-codoped ZnO-NCs and antioxidant of ZnO-NPs and P and N-codoped ZnO-NCs.
- To study the kinetic of MB dye degradation using ZnO-NPs and P and N-codoped ZnO-NCs.

1.4. Significance of the study

Nanotechnology and its application are hot research areas in modern sciences. This work is one of the modern science inputs that will undergo synthesis and characterization of Phosphorus and Nitrogen-codoped Zinc Oxide Nanocomposite useful in photocatalysis, antibacterial and antioxidant activities. There are many advantages to the accomplishment of this study for the science world, environmental management, and pharmaceutical and human health protection.

ZnO-NPs have attracted great interest in antimicrobial activity due to their large surface area, high sensitivity, mechanical strength, and selectivity to the target ion, and also good electrocatalytic activity. Therefore, this study is important in the modification of antimicrobial agents that already exist to improve antimicrobial and photocatalytic activity. Developing Nitrogen and Phosphorus codoping ZnO-NCs antimicrobial agents is an attractive and cost-effective means to overcome drug resistance problems.

Generally, the significances of this study are:-

- In health and modern science, for the development of photocatalytic, antioxidant, and antibacterial agents for pharmaceutical and human health protection.
- Environmental protection is for the removal of contaminated wastewater from the environment.
- To give some additional information for other research on this area.

2. RELATED LITERATURE REVIEW

2.1. Water Pollution and Human Health

Progressively, an increase in industrialization as well as an increase in population has created an amazing increase in water contamination [17]. Water is especially polluted by organic and inorganic pollutants which are extremely released from the industries as indicated in **Figure (1)** [18]. Nanotechnology could be an effective tool in studying with removal of contaminations [19]. Numerous studies show that the incorporation of nanoparticles with accepted analysis could increase the effectiveness of pollutant cleaning. Competent wastewater treatment is important for economic growth in the modern time of water and water resources inadequacy [20]. Wastewater treatment is the most necessary for health in this world full of industries [13]. Among various treatment methods, current improvements in the field of nanotechnology have gained the essential of scientists. Different proper techniques (such as coagulation, flocculation filtration fluoridation, etc.) have been aids for water cleaning by identifying the pollutants, but these technologies are ineffective and cheap. Nanotechnology is one of the most significant tendencies in science and is recognized as one of the essential technologies of the present century. The most interesting characteristic of nanomaterials having a high surface area that can be used efficiently to clear away toxic metal ions and inorganic and organic solutes from the water. A large number of photocatalyst applications are indicated. The most essential oxide metal oxides are TiO_2, Fe_2O_3, SnO_2, ZrO_2, GeO_2, Sb_2O_3, V_2O_5, WO_3, Cu_2O and In_2O_3, etc. [21–23].

Figure1. *The Affected water body by organic dyes that are released from different industrial products which cause harmful effects of water remediations.*

In an optimal photocatalytic process, organic pollutants are mineralized into carbon dioxide (CO_2), water (H_2O), and mineral acids in the presence of ZnO particles and reactive oxidizing species, such as oxygen or air. The photocatalytic reactions were initiated when the ZnO particle absorbs photons with energies higher than that of its band gap energy from the illumination. In this way, a photo-induced electron is promoted from the valence band (VB) to the conduction band (CB), forming a positive hole (h^+_{VB}) and electron (e^-_{CB}) on the surface of the ZnO particle. It should be noted the photo-generated holes in the valence band will recombine with the photo-excited electrons in the conduction band and dissipate in the form of heat. Therefore, the presence of oxygen as electron scavengers prolongs the recombination of electron-hole pair while forming the superoxide radicals $\cdot O_2^-$. Their action of h^+_{VB} with OH^- may lead to the formation of hydroxyl radicals. The hydroxyl radical is an extremely strong, non-selective oxidant (E^0=+3. 06V) which leads to the partial or complete mineralization of organics. Moreover, the high oxidative potential of the hole in the photocatalyst also permits the direct oxidation of organic matter to reactive intermediates as shown in **Figure 2**. The superoxide radicals were further protonated to produce hydroperoxyl radical (HOO·) and subsequently H_2O_2. The $HOO^{\cdot}$ also functions as an electron scavenger to trap conduction band electrons which further delay the recombination process. The general photocatalysis mechanism processes are shown in **Figure 2.**

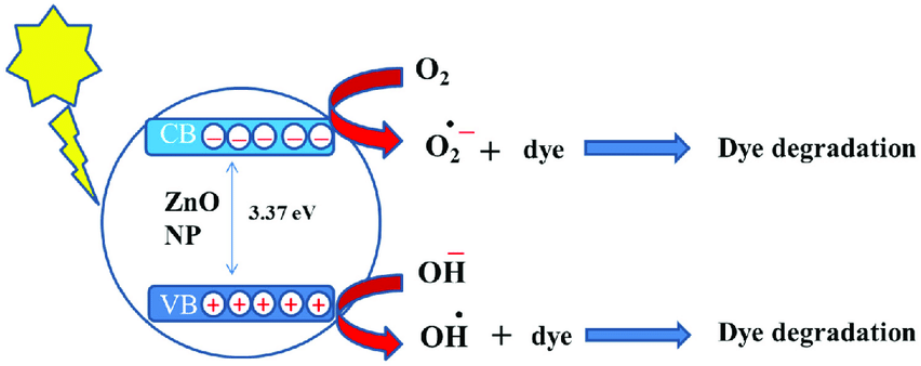

Figure.2: *The photoexcitation of the dye followed by its photocatalytic degradation under solar irradiation.*

Anionic dopants ZnO-NPs the number of oxygen vacancies sense an important role in influencing the photoactivity of non-metals doped ZnO system [24]. During the photocatalytic process, the oxygen vacancies and deformity become centers to trap photogenerated electrons. Accordingly, the electron-hole rearrangement process is hindered [25]. Therefore, the higher the quantity of oxygen defects, the better the photocatalytic activity. Prepared non-metals doped ZnO by precipitation method and established that the interrupting of the non-metal dopants with ZnO crystallization resulted from the photoactivity by enhancement in light absorption and was more effective in transferring electron-hole. Doped ZnO nanostructures an intrinsically n-type semiconductors due to the variation from stoichiometry and the presence of intrinsic deformity such as oxygen vacancies (VO), zinc interstitials (Zni), and zinc vacancy (Vzn) [26]. Doped ZnO can be predicted to exhibit better optical properties, high luminescence properties, and high photocatalytic activity in the removal of organic contaminants. This could be due to the increased particle surface area, reduced band gap energy, improved adsorption ability of the particle surface, and dopant ZnO interfaces. The n-type doping of ZnO with a donor state is accomplished by substituting atoms with one or more electrons in the outer shell compared to the replaced element (Zn or O) in ZnO [27, 28]. Consequently, the substitution of group-III elements on Zn sites and group-VII elements on O sites creates highly conductive n-type ZnO. The p-type doping of ZnO with an acceptor level is created by replacing group-I elements on Zn sites and group-V on O sites. Although, ZnO can be easily n-type doped, attempts to acquire faithful p-type doping are now an obstacle due to the low solubility, much higher ionization, and formation energy of p-type dopants. Doped zinc oxide nanomaterials mark the removal of extremely toxic dyes and pathogens from water, and thus hold promise for protecting ecological and human

health. In particular, it offers good prospects as a transparent conductive oxide when doped with several types of dopants such as Nitrogen (N) and Phosphorus (P). Synthesis of ZnO nanoparticles and study of the influence of Nitrogen and phosphorus doping with different concentrations on the structural, morphological, and optical properties of ZnO nanoparticles. Doping in ZnO causes the narrowing of the band gap in ZnO and increases the absorption of visible light.

Co-dopants of ZnO-NPs The speed reconnection of the electron-hole pairs can also be responded to by the presence of co-dopants [21]. It can be observed that the Nitrogen and Phosphorus co-doped ZnO has been applied in reducing dye removals, such as Methylene Blue [29]. The photodegradation effects of Phosphorus and Nitrogen co-doped ZnO are greater than undoped ZnO and single-dopant ZnO systems [4, 15]. This is due to the Nitrogen and Phosphorus co-doped will continuously trap the photogenerated electron from the conduction band of the ZnO and as a result decrease the reconnection speed of the electron-hole. Therefore, the photoinduced generation of electron-hole pairs will proceed and make a quantity of large active superoxide radical anions and hydroxyl radicals which improves the photodecomposition effects of the dyes. Nitrogen and Phosphorus Codoped ZnO is appropriate for optoelectronic devices since they have suitable transparency in the visible region, tunable band gap, and low resistivity [6]. Additionally, Nitrogen and Phosphorus Codoped ZnO advanced in antibacterial activity and water decontamination, resulting in improved photocatalytic activity [30, 31]. Nitrogen and Phosphorus Co-doped ZnO indicates a great tendency for the degradation and removal of environmental contaminants [29, 32]. Nanomaterials give marks effective for the localized antibacterial action, and their degradation is found to be faster [33]. Furthermore, the ionic radius creates charge inequality and hence enhances photocatalytic and antibacterial activity [34, 35].

2.2. Nanomaterial and Nanocomposite

Nanomaterials are materials with at least one dimension in nanometers (<100 nm) whereas Nanoscience is the study of the properties of matter at the nanoscale. Nanotechnology is increasingly exploited in science and technology and has become a part of modern technology, which, at present, can be determined “a key technology of the 21st century”. Nanoscience and nanotechnology involve the preparation, assembly, manipulation, and application of materials

characterized by at least one size in the nanometric range, some of these nanomaterials being found in products available in our daily lives [36]. Due to their improved chemical and biological reactivity, they may easily interact with cells and microorganisms inducing or enhancing existent properties. The various physical parameters of nanoscopic materials that control the chemical, physical, electronic, and optical properties are shape, size, and surface morphology [37, 38]. nanomaterials have found different applications in the fields of photonics, energy storage, drug delivery, catalysis, fuel cells, Nano-medicines, etc. Properties of nanomaterials the nanoparticles have more surface area and some unique properties compared with bulk materials. The properties of nanomaterials are expressed in terms of mechanical properties, and physical and chemical properties. Metal and metal oxide nanoparticles are extensively evaluated in medicine, water pollution protection, energy, electronics, etc. ZnO a transition metal oxide with a wide band gap of 3.37 eV is a promising p-type material with physiochemical properties strongly dependent upon its morphology and size. Zn is a relatively low-cost metal that is more cost-effective than Au and Ag. Additionally, ZnONPs are efficient catalysts, with high yields and easy product separation, and they can be reused repeatedly. Zn nanoparticles can be easily oxidized to form Zinc oxides (ZnO), which are inorganic NPs. Both Zn and ZnO NPs are used extensively as anticancer, antimicrobial, photocatalytic, and antioxidant agents [39].

Nanocomposites formed by a phase-dispersed nanomaterial and a polymeric host matrix are highly attractive for nano- and micro-fabrication. The combination of nanoscale and bulk materials aims to achieve an effective interplay between extensive and intensive physical properties. Nanocomposites are substances that incorporate nanoparticles (0.5-5% by weight) into a matrix of standard material, which enhances the mechanical strength and toughness including thermal or electrical conductivity and other properties. Nanocomposites are versatile in terms of their applications such as anti-corrosive, healing of bones, sensors, environmental protection, wastewater treatment, diagnosis of tumors, and other diverse uses. A Nanocomposite is a framework for nanoparticles that are incorporated to improve a specific property of the material. In the present era, the perception of acquiring design uniqueness and property combinations that are not found in conventional composites is obtained by using nanocomposites.

2.3. Preparation of ZnO nanoparticles

The investigation of zinc oxide nanoparticles has increased due to their broad applications in solar cells, photovoltaic, drug delivery systems, gas sensors, field emission devices, coating, electrochemical, antibacterial, capacitors, and cosmetics [40]. ZnO is an n-type semiconducting metal oxide (SMO) having piezoelectric and pyroelectric characteristics, long life, as well as high sensitivity to various target gases [40]. The ZnO nanoparticles present different semiconducting features as they possess high exciton bonding energy and a wide bandgap with 60 meV and 3.37 eV, respectively. These characteristics have made ZnO important to extensively delegate as a gas sensing material in houses and industrial environments to protect against toxic, harmful, explosive, and greenhouse gases and for air quality assessment. The ZnO NPs can have different morphologies such as nanoflower, nanorod, nanoflake, nanobelt, nanosheets, and nanowire [10, 41].

2.4. Chemical properties of ZnO-NPs

ZnO is a wide band-gap semiconductor with a large exciton binding energy of 60 meV at room temperature. The electrical, optical, and magnetic properties of ZnO can be improved by the use of ZnO on the nanoscale ZnO is an environmentally friendly material as it is compatible with living organisms, which lends itself nicely to a broad range of daily applications that will not leave any risks to human health, and environmental impacts. ZnO has received much attention in the degradation and complete mineralization of environmental pollutants. Since ZnO has almost the same band gap energy as TiO_2 (3.2 eV), its photocatalytic capability is anticipated to be similar to that of TiO_2. Moreover, ZnO is relatively cheaper compared to TiO_2 whereby the usage of TiO_2 is uneconomic for large-scale water treatment operations. The greatest advantage of ZnO is the ability to absorb a wide range of solar spectrum and more light quanta than some semiconducting metal oxides. The major drawbacks of ZnO are the wide band gap energy and photo corrosion. The light absorption of ZnO is limited in the visible light region which is due to its wide band energy. This results in rapid reconnection of photogenerated charges and thus causes low photocatalytic efficiency.

2.5. Chemical Synthesis of Zinc Oxide Nanoparticles

Generally, two main methods are considered for the preparation of NPs: the top-down and the bottom-up methods. The top-down method refers to the breaking down of larger materials into

smaller nanosized particles. On the other hand, in the bottom-up method, smaller units such as atoms and molecules are used to create NPs. The various methods that have been used since previous periods for the preparation of ZnO-NPs are microwave-assisted combustion, thermal decomposition, sol-gel method, and hydrothermal methods. However, the latest techniques used for the preparation of ZnO-NPs are ultra-sonication, co-precipitation, and green synthesis.

2.5.1. Sol-gel method ZnO-NPs synthesis

Well-known liquid phase techniques used for manufacturing homogeneous metal oxides. The sol-gel synthesis process of nanoparticles was released to form an inorganic compound through the chemical reaction of a certain solution. According to the reaction procedure, the sol-gel method can be classified into two kinds. In the reaction medium, the hydrolytic sol-gel method, if water is used as the solvent, and the non-aqueous sol-gel process if organic solvents such as alcohol, ether, and ketone are used as a reaction medium to produce oxygen. Still now, instead of water and alcohol, a base and an acid are also being used for the hydrolysis of metal alkoxide (sol-gel). Among all, the precursor's metal alkoxides are considered the best because of their easy purification and very good solubility [42]. The process consists of 5 steps namely, hydrolysis, condensation, aging, drying, and calcination. This method has been broadly used because the yield acquired consists of a large surface area, a high porous level, and its ability to stabilize heat equilibrium. The uses of the sol-gel method are to produce a good rate of thermal stability, high mechanical stability, good solution resistance, and the possibility to stimulate change. Sol-gel and calcination method for the preparation of desired product of ZnO nanoparticles. Nano zinc oxides produced under these conditions were characterized based on crystal form, as well as the morphology and particle size [43].

2.5.2. Vapor Transport method for ZnO-NPs synthesis

The vapor transport process is the most known method for the preparation of ZnO nanostructures. In this method, zinc and oxygen or oxygen mixture vapors are transported and react with each other resulting in the formation of ZnO nanostructures. There are various ways to generate Zn and oxygen vapor. Decomposition of ZnO is an easier, direct, and easy method; however, it is limited to very high temperatures such as ~ 1400 ℃. Another direct method involves heating of zinc powder under the flow of oxygen. It involves a relatively small growth temperature (500~700℃), but the ratio between the Zn vapor pressure and oxygen pressure must

be carefully controlled to obtain the desired ZnO nanostructures. It has been observed that the change in this ratio results in a large variation in the morphology (size and geometry) of nanostructures.

2.5.3. Hydrothermal method for ZnO-NPs synthesis

The hydrothermal method is an inexpensive, highly efficient, and widely used technique for the production of single crystalline metal oxide NPs from its aqueous precursor solution under high temperature and pressure using an autoclave. Due to the temperature gradient established between the two ends of the growth chamber, the materials get dissolved at the hotter end and deposited on the seed crystal the at cooler end. Finally, the precipitates were collected, washed and oven dried [10].

2.5.4. Co-precipitation method for ZnO-NPs synthesis

The co-precipitation method is the most convenient, facile, and cost-effective approach for the production of several metal oxide NPs with high yield and purity. In this method, the precursor solution (metal salts) is first treated with a precipitating agent (alkali) to obtain the precipitates which are further washed to remove impurities and dried to get solid powder. Sometimes, the formed metal hydroxides are calcined to get metal oxide NPs. synthesized quasi-spherical ZnONPs with 60 and 50 nm average size by co-precipitation method using zinc nitrate hexahydrate in ethanol as a precursor and KOH or NaOH as precipitating agents respectively.

2.5.5. Microwave-assisted combustion method ZnO-NPs synthesis

Microwave (MW)-assisted combustion is a fast, energy and time-saving process for the production of several metal oxide NPs with higher selectivity and chemical yield. In this method frequency electric fields are used for heating dipolar materials which are forced to align with the MW electric field. This rapid reorientation of molecules will produce a large amount of heat by the friction of the molecules during their movement within a very short time.

2.5.6. Green synthesis of NPs method for ZnO-NPs synthesis

Provides a simple, cost-effective, and eco-friendly approach for the synthesis of several types of NPs with higher reproducibility and stability [44]. Green synthesis is an emerging field that uses environment-friendly and bio-safe reagents with the release of nontoxic chemicals [45]. There are three major types of biological materials such as microorganisms, bio templates, and plant

extracts which are used for biosynthesis of NPs [46]. In microorganism-assisted biosynthesis, metal nanoparticles are formed by the reduction of the corresponding metal salts using microbial enzymes secreted from microorganisms like bacteria, yeast, and fungi. There are mainly two types of microbial reduction; (i) intracellular synthesis, where metal ions are transferred into microbial cells, and (ii) extracellular synthesis, where the cell surface holds the metal ions and reduces them.

2.6. Advantages of Chemical Synthesis.

Chemical preparations are one of the most essential methods that can be obtained by using optimization of precursors and under various states like temperature, time, the concentration of reactants, and so forth. The difference in these parameters indicates morphological variations in the size and geometries of determined nanoparticles.

2.7. Chemical Reaction of Zinc Metal with Alcohol.

Mostly alcoholic media like ethanol, methanol, or propanol are used for the chemical synthesis of ZnO nanoparticles. Typically in this synthesis 5 mg of zinc metal powder is added to 10 mL of ethanol. Further, this reaction mixture is sonicated for 20 minutes transferred into a stainless steel autoclave, and sealed under inert conditions. The reaction mixture is heated slowly (2 ℃ to 200 ℃ per minute) and maintained at this temperature for 24 to 48 hours. The resulting suspension will then be centrifuged to retrieve the product, washed, and then finally vacuum dried. In alcoholic media growth of oxide particles is slow and controllable [33].

2.8. Application of ZnO-NPS

Literature reports suggest two main mechanisms responsible for antibacterial activity. The first is the activation of ZnO-NPs by light, resulting in a series of reactions leading to the formation of reactive oxygen species (ROS) such as hydrogen peroxide (H_2O_2), superoxide anion radical (O_2•-), hydroxide radical (HO_2•), and hydroxyl radical (HO•). The formation of ROS in the internal and external environment of the bacterial cell, as well as their accumulation in the cell, leads to damage to many structures resulting in cell death. The mechanism of action in the dark is associated with the dissolution of these nanoparticles, which leads to an increase in the concentration of Zn^{2+} ions in the bacterial cytoplasm and the cell environment. ZnO-NPs can

also act by direct contact of the tested particles with the cell, as a result of which the bacterial walls are damaged and disorganized, and the cell membrane becomes more permeable, making nanoparticles easier to enter the bacterial cytoplasm.

2.8.1. Antimicrobial activity

The minimum inhibitory concentration (MIC) was sufficient to prevent bacterial growth in vitro and the lowest concentration of ZnO nanoparticle suspension resulted in a reduction of initial inoculum. There is a huge divergence in effective bactericidal doses [47]. There is no clear relationship between cytotoxicity and ZnO size; it seems that the action of ZnO-NPs is primarily dependent on the method of nanoparticle synthesis and the resulting surface charge effects. However, it can be seen that within the same type of ZnO-NPs, smaller particles are more effective [48]. It is a promising alternative to traditional chemical synthesis ensuring greater antimicrobial effectiveness and greater safety for the environment. Gram-positive bacteria are more sensitive to ZnO-NPs than Gram-negative bacteria Furthermore; prolonged exposure to ZnO-NPs can lead to the adaptation of bacteria and reduce the effectiveness of nanoparticles [49].

2.9.1. Photocatalytic Degradation

The term photocatalysis consists of the combination of photochemistry and catalysis. It implies that light and a catalyst are necessary to bring about or accelerate a chemical transformation. In other words, photocatalysis can be defined as the “acceleration of a photoreaction in the presence of a catalyst”. This definition includes photosensitization, i.e. a process by which a photochemical alteration occurs in one chemical species as a result of initial absorption of radiation by another chemical species called the photosensitizer. It follows from the above that heterogeneous photocatalysis involves photoreactions that occur at the surface of a catalyst [50]. If the adsorbate is photoexcited first and then interacts with the ground state of the catalyst substrate, the process is referred to seen then interacts with the ground state of the catalyst substrate; the process is referred to sensitized photoreaction. On the other hand, if the catalyst is photoexcited first and then interacts with the ground state adsorbate molecule, the process is a “catalyzed photoreaction”. In most cases, heterogeneous photocatalysis refers to semiconductor photocatalysis or semiconductor-sensitized photoreaction. The basic reactions that occur during the photocatalysis process are given by **equations (1-5)** [17].

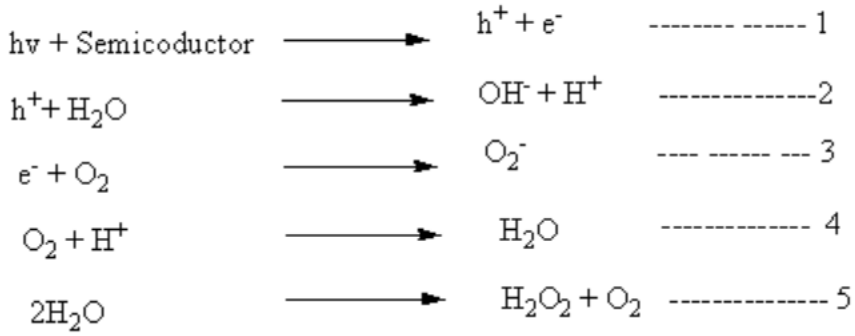

2.9.2. Medicinal uses

ZnO nanoparticles play some potential role in the CNS (central nervous system) and perhaps during the development processes of diseases through mediating neuronal excitability or even the release of neurotransmitters. Some studies have indicated that ZnO affects the functions of different cells or tissues, biocompatibility, and neural tissue engineering [51].

2.9.3. Agriculture uses

Zinc oxide nanoparticles have prospective potential to boost the yield and growth of food crops. Seeds were treated with different concentrations of zinc oxide nanoparticles enhanced seed germination, seedling vigor, and plant growth and these zinc oxide nanoparticles also proved to be effective in increasing stem and root growth in seeds. They observed the effect of chemically synthesized Zinc oxide (ZnO) nanoparticles in biological systems. When ZnO was applied at various concentrations [52].

3. MATERIALS AND METHODS

3.1. Description study area

This study was conducted at Jimma University College of Natural Science Analytical and physical Chemistry Laboratory to Synthesize and characterization of ZnO-NPs, N-doped ZnO-NPs, P-doped ZnO-NPs, and P and N-cooped ZnO-NCs for photocatalytic degradation Methylene Blue, Antimicrobial and antioxidant activities.

3.2. Chemicals and Instruments

Chemicals used for this research are sodium hydroxide (NaOH) ≥ 98% Blulux Laboratories Ltd - 121005), Ethanol (CH_3COH) (purity ≥ 99%), Zinc Nitrate hexahydrate ($Zn(NO_3)_2.6HH_2O$ ≥ 98% (Loba Chemie Pvt. Ltd), Urea (NH_2CONH_2), Ammonium dihydrogen phosphate ($(NH_4)(H_2PO_4)$), Nitric acid (HNO_3), Hydrochloric acid (HCl), Potassium nitrate (KNO_3) and distilled water. Different laboratory instruments were used, Beakers, Magnetic stirrer, Electronic balances, pH meters, Spoons, Sample bottles, Measuring Cylinders, Pipettes, Burettes, Funnels, Watman Filter paper, Muffle furnace, Oven, Crucible, and measuring XRD-7000, Cu kα (λ=1.54178 Å) radiation, UV-Vis (SPECORD 200 PLUS -223E118F), and FT-IR (PerkinElmer Spectrum 2, Wavenumber range (8300-350 cm^{-1}) and SEM were used in this research.

3.3. Synthesis of Zinc Oxide Nanoparticles (ZnO-NPs)

Zinc Oxide Nanoparticles (ZnO-NPs) were prepared from Zinc Nitrate hexahydrate ($Zn(NO_3)_2.6H_2O$ using the Sol-gel method [42]. 3.5 grams of zinc Nitrate hexahydrate was dissolved in 25 mL of distilled water at room temperature. The next 0.5 grams of Sodium hydroxide was dissolved in 25 mL of distilled water at room temperature. Both solutions were stirred with constant stirring for 1 hour with a magnetic stirrer. Then Zinc Nitrate hexahydrate Zn $(NO_3)_2.6H_2O$) solutions were continuously stirred and sodium hydroxide (NaOH) solutions were added drop wise and carefully recorded any change observed during the synthesis and kept further pH optimization of the solution ranged between 8-12 at room temperature and the reaction, until white milky precipitate a gel-like product was formed and the desired product was obtained by characterizing UV-Vis at optimum pH was 11. The solution was centrifuged at 5000 rpm for 10 minutes washed with distilled water and ethanol and was dried and kept for further

calcination at different temperatures 200 ℃, 300 ℃, 400 ℃, and 500 ℃. Then the desired product ZnO-NPs was obtained at 300 ℃.

3.3.1. Synthesis of Phosphorus doped Zinc Oxide Nanoparticles (P-doped ZnO-NPs)

ZnO-NPs prepared at 300 ℃ were prepared for doping. The selected phosphorus-doped zinc oxide nanoparticles (P-doped ZnO-NPs) were prepared from 7 % Ammonium dihydrogen phosphate ($(NH_4)(H_2PO_4)$) were dissolved in 10 mL distilled and stirred for 1 hour and 93 % zinc oxide nanoparticles were dissolved in 10 mL DW and stirred for 1 hour. Then the two solutions were mixed and stirred for 2 hours. The solution was centrifuged at 5000 rpm for 10 minutes washed with DW and ethanol then the precipitate was dried in an oven at 50 ℃ for 1 hour. After being dried, the white powder was calcined in a muffle furnace for 3 hours at 300 ℃ and called P-doped ZnO-NPs.

3.3.2. Synthesis of Nitrogen-doped Zinc Oxide Nanoparticles (N-doped ZnO-NPs)

N-doped zinc oxide nanoparticles were prepared from ZnO-NPs at 300 ℃ were synthesized for doping [53]. The selected Nitrogen-doped Zinc Oxide Nanoparticles (N-doped ZnO-NPs) were prepared from 3 % Urea (NH_2CONH_2) [38] were dissolved in 10 mL DW and stirred for 1 hour and 97 % zinc oxide nanoparticles were dissolved in 10 mL DW and stirred for 30 minutes. Then the two solutions were mixed and stirred for 1 hour. The solution was centrifuged at 5000 rpm for 10 minutes washed with DW and ethanol and the precipitate was dried in an oven at 50 ℃ for 1 hour. After being dried, the white powder was calcined in a muffle furnace for 3 hours at 300 ℃ and called N-doped ZnO-NPs [55].

3.3.3. Synthesis of Phosphorus and Nitrogen-codoped Zinc Oxide Nanoparticles (P and N-codoped ZnO-NCs)

Nitrogen and Phosphorus-codoped zinc oxide nanoparticles were prepared by dissolving 90% ZnO-NPs, 3% N, and 7% P in 10 mL of distilled water and stirring for 1 hour. The solution was centrifuged at 5000 rpm for 10 minutes and washed with DW and ethanol and the precipitate was dried in an oven at 50 ℃ for 2 hours. After being dried, the white powder was calcined in a muffle furnace for 3 hours at 300 ℃ and called P and N-codoped ZnO-NCs.

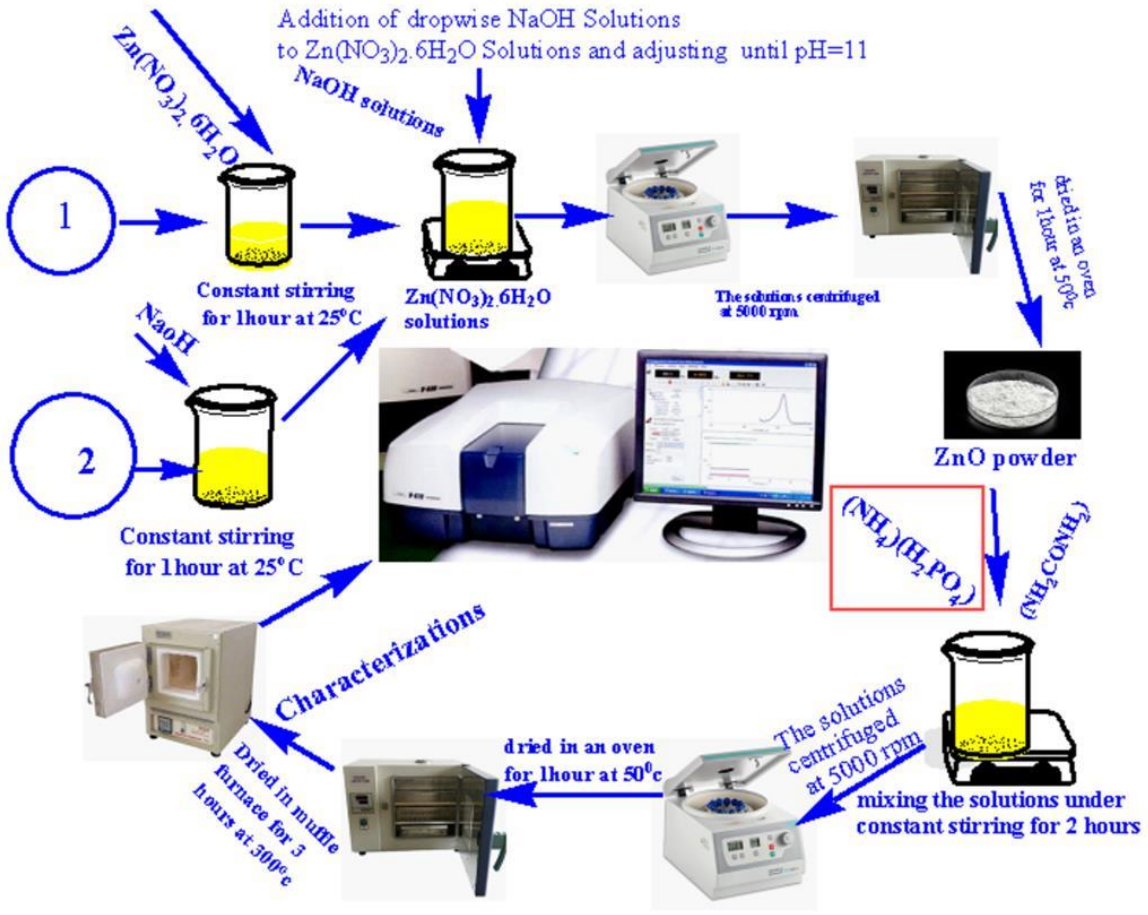

Figure 3*. Schematic Representations of the Synthesis of pure ZnO-NPs, N-doped ZnO-NPs, P-doped ZnO-NPs and P and N-codoped ZnO-NPs*

3.4. Characterization

The prepared samples of pure ZnO-NPs, P-doped ZnO-NPs, N-doped ZnO-NPs, and P and N-codoped ZnO-NPs were characterized by using UV-Vis spectrophotometer FT-IR, XRD and SEM. 0.1M Solutions of ethanol were used to specify the characterization of UV-Vis measurements whereas FT-IR, XRD, and SEM were used to characterize by using their solid powders. Crystal structure and phase composition of prepared samples were resolved by using X-ray diffraction (XRD) at a voltage of 40 kV, filament current of 30 mA, and Cu Kα1 radiation (λ=1.5418 Å) in the 2θ ranges from 10°- 80°. We used a UV-Vis spectrophotometer to evaluate the band gap energies and take absorbance measurements. The chemical composition of the sample was investigated using Fourier transform infrared (FT-IR) in the wavenumber range from

4000-400 cm^{-1}. Scanning electron microscopy (SEM) was also used to survey the samples' morphologies and microstructures.

3.5. Photocatalytic experiments

Photocatalytic degradation of ZnO-NPs and P and N-codoped ZnO-NCs were examined by using MB aqueous solution to direct solar radiation in October between 05:00 AM - 08:00 AM. The average daily temperature (Jimma) was 29 ℃ to 31℃. The solutions were stirred by using the magnetic bar in the dark for 30 minutes to accomplish adsorption-desorption equilibrium between the photocatalyst and the dye's earlier radiation. The photocatalytic degradation of MB was examined using different concentrations of the photocatalyst in the stock solution of 500 mg/L of the MB dye in Distilled water [13]. Based on UV-Vis measurement at the suitable wavelength, the elimination or removal efficiency of MB was determined.

3.6. Point zero charge (PZC)

PZC is the net surface charge of adsorbent is equal to zero. At that pH, the charge of all positives becomes equal to the negative one. The point zero charge is acquired by acid-base titration of the colloidal dispersions while observing the electrophoretic ability to move the particles and the pH of the suspension PZC was determined by salt addition methods, taking a solution containing 0.1M KNO_3. Set the different pH values 6, 8, and 9 of the solution by titrating 0.1M NaOH and 0.1M HCl by using a pH meter. Then in each three flasks of adjusted pH, add the 0.1g of P and N codoped ZnO-NCs and record the initial pH (pHi). Each solution in the flask was shaken by using a sonicator for 3 hours at room temperature of 25 $°c$. After the equilibrium each flask solution was separated and pH final (pHf) was again recorded. Then the point of Zero Charge ($\Delta pH = pHi - pHf$) was determined [15].

3.7. Antioxidant activity

ADPPH is a stable free radical that can be used to measure the radical scavenging activity of the tendency of ZnO-NPs antioxidants. The NPs' tendency to inhibit oxidation was evaluated by bleaching out or depriving of color-performing methanol solution of DPPH [55]. In methanol, DPPH produces a violet or purple color that disappears to yellow in the presence of antioxidants. A solution of 0.1 μM DPPH in methanol was mixed with 1mL of pure ZnO-NPs and P and N-codoped ZnO-NCs in methanol at concentrations 5, 10, 20, 40, and 80 mg/mL for each

nanoparticle. The mixture was culminated and incubated in the dark at room temperature for 30 minutes. Using a spectrophometer the absorbance of the mixture at 517 nm was evaluated to examine the percentage of DPPH radical scavenging activity. Ascorbic acid was providing as standard by **equation (6)** [5, 33].

$$\% \text{ DPPH radical scavenging activity} = \frac{A0 - A1}{A0} \times 100 \text{ ---------- (6)}$$

The experiment was performed two times at each concentration, and the IC_{50} was evaluated by scheming the percentage inhibition against the concentration, A_O representing the control absorbance, and A_1 representing the sample absorbance.

3.8. Antimicrobial activity

The antimicrobial activity studies were organized in the Jimma University Biology Department Laboratory using the agar disc diffusion methods. The biological evaluating results of prepared nanoparticles were examined against bacterial strains, including, Bacillus cereus, staphylococcus aureus, salmonella typhus, and Escherichia coli. Antifungal activity was also examined against Candida albcans. A culture with test tubes of approximately equal concentration or density of 0.5 McFarland standard was used for media inoculation (55 Test bacteria and fungi were ZnO-NPs, P-doped ZnO-NPs, N-doped ZnO-NPs and P and N-codoped ZnO-NPs agar respectively, using freshly grown liquid cultures with similar turbidity to 0.5 McFarland. The negative control was DMSO while Gentamycin and Clotramazole (ant-fungal) were used as positive control for bacteria. An ample solution containing 100 mg/mL of each tested compound was prepared by dissolving them in DMSO. The solution was loaded onto the wall of the culture and incubated at 37 °C for 24 hours. Inhibition Zones developed on the plate around the standard paper disc with a diameter of 6mm, and the antimicrobial activity of nanoparticles was established by measuring the diameter of the zone inhibition growth around the sample [47].

4. RESULTS AND DISCUSSIONS

4.1. Characterizations

The synthesized ZnO-NPs, P-doped ZnO-NPs, N-doped ZnO-NPs, and P and N-codoped ZnO-NCs obtained well-known sol-gel methods were characterized by using instruments such as UV-Vis, XRD, FT-IR and SEM. Light absorption characteristics of ZnO-NPs, P-doped ZnO-NPs, N-doped ZnO-NPs, and P and N-codoped ZnO-NCs have been done by spectrophotometer [9]. **Figure 4** indicates that the combination of P-doped ZnO-NPs, N-doped ZnO-NPs, and N &P - Codoped into the pure ZnO-NPs resulted in absorbance shifts towards red. Optimizations of the amount of P and N-codoped ZnO-NCs needed to bring maximum shift were also obtained. Correspondingly, it was found that the combination of 10% P and N-codoping into the pure ZnO-NPs shifted the wavelength of the maximum absorbance from 374 nm to 380 nm. This change is conducted by the surface charge of nanoparticle evaluation and crystallinity [14].

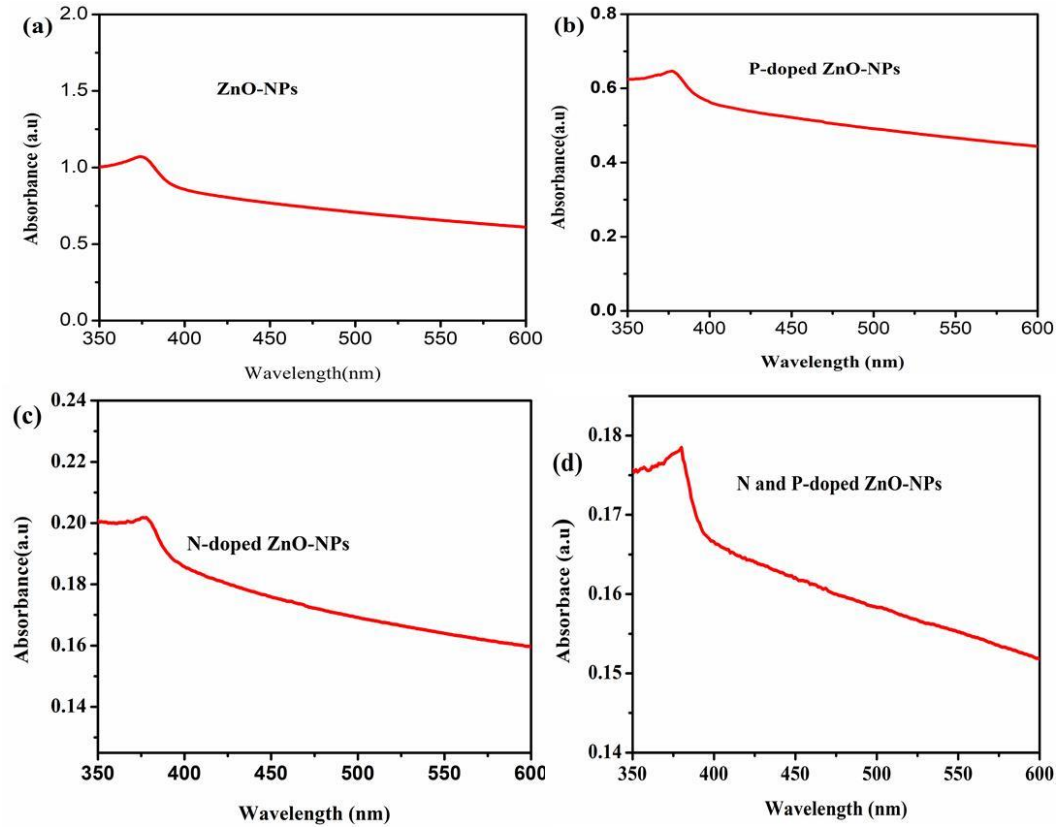

Figure 4. *UV-Vis Absorption spectrum of (a) ZnO-NPs, (b) P-doped ZnO-NPs, (C) N-doped ZnO-NPs, and (d) N and P-Codoped ZnO-NCs.*

The values of logA, α, $h\nu$, and $(\alpha h\nu)^2$ were measured from UV-Vis data to examine the band gap energies for all samples. **Figure 5** indicates that the function of $(\alpha h\nu)^2$versus photo energy ($h\nu$) for ZnO-NPs, N-doped ZnO-NPs, P-doped ZnO-NPs and P and N-Codoped ZnO-NCs. As a result, the approximate optical band gap of ZnO-NPs from 2.92 eV **Figure 5(a**) to 2.53 eV **Figure 5(d).** The reduction of the band gap energy could be assigned to the effect of the combination of the P-doped ZnO-NPs, and N-doped ZnO-NPs into pure ZnO-NPs that make better the surface charge and stability of the Nanomaterials.

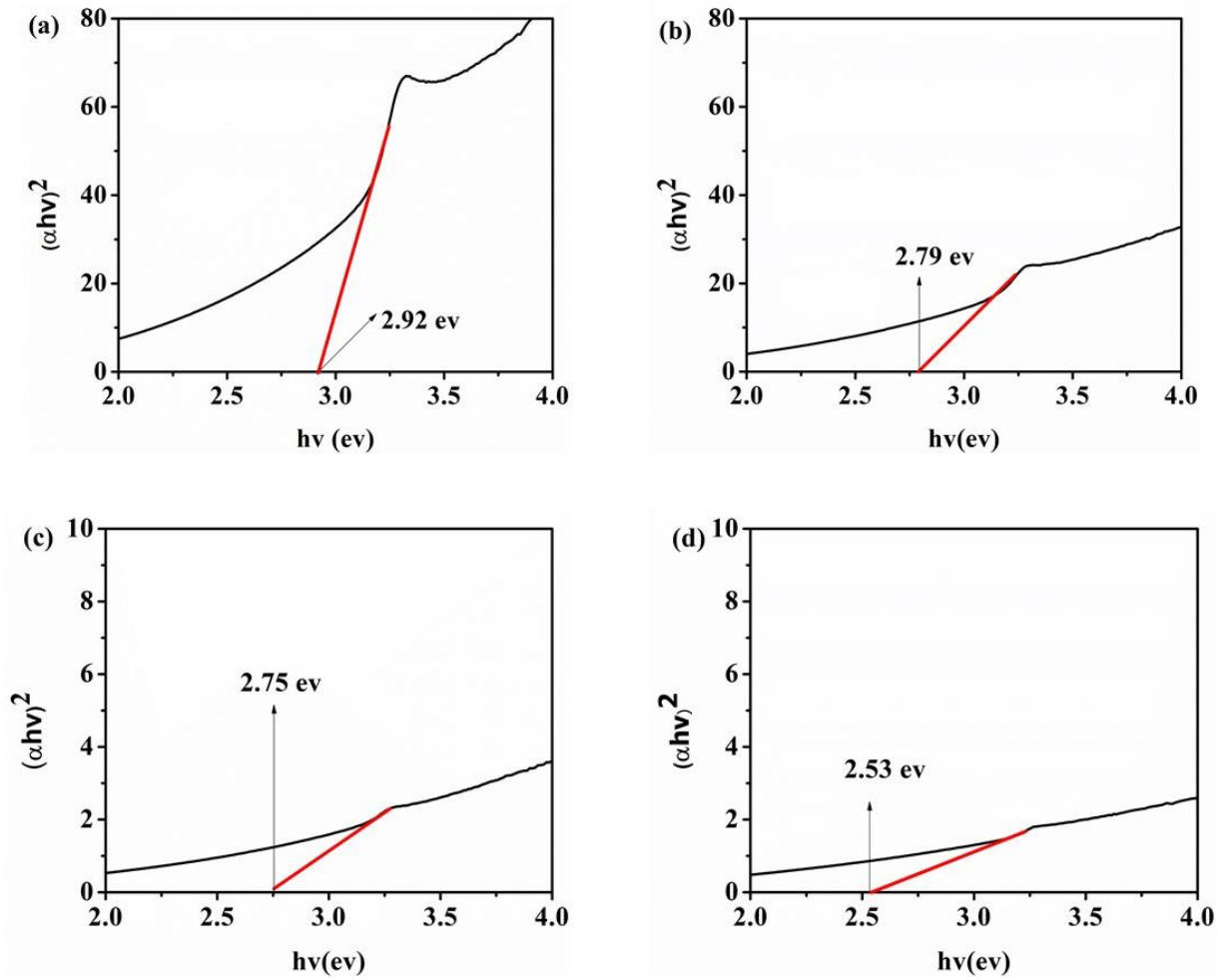

Figure* 5.The energy band gap of (a) ZnO-NPs, (b) P-doped ZnO-NPs, (c) N-doped ZnO-NPs, and (d) P and N-codoped ZnO-NCs.*

The XRD diffraction results in **Figure 6** indicate a pattern that competes with the standard of ZnO-NPs provided by the (JCPDS card number 36-1451). This result indicates the hexagonal wurtzite structure of the studies ZnO-NPs with spatial group P-doped ZnO-NPs, N-doped ZnO-NPs, and its P & N-Codoped ZnO-NCs as specified in the (JCPDS card number 36-1451) [11, 57]. The X-ray Diffraction analysis determines the detailed finding on the structural properties and approves peak position intensity, peak intensity, and full-width half maximum (FWHM) data. The nanoparticles showed high purity levels as peaks of any other phase identified [7] by taking into consideration, that distinctly identified peaks were at (2θ)=29°, 31. 2°, 32°, 33°, 34.6°, 36.7°, 42.7°, 47.8°, 50.8°, 57°, 60.8°, 63. 1°, 68.2° and 69.6°. The addition of amorphous P-doped and N-doped did not change the crystalline nature of ZnO-NPs. This is indicated by similar diffraction patterns of P and N-codoped ZnO-NCs and hexagonal ZnO (JCPDS card number 36-1451), which are the same as those of pure ZnO [58, 59]. There is no recognition of P-doped ZnO-NPs and N-doped ZnO-NPs diffraction found in the composite due to the low convenient and amorphous features of P-doped ZnO-NPs and N-doped ZnO-NPs. The composites show characters' diffraction peaks similar to those of ZnO-NPs. Showing a low effect of P-doped ZnO-NPs and N-doped ZnO-NPs changes on ZnO Crystallinity [60].

The diffraction peaks were shifted the two theta values and the crystalline size of ZnO-NPs, P -doped ZnO- NPs, N-doped ZnO-NPs, and P and N-Codoped ZnO-NCs catalysts were calculated from highest intensity diffraction peaks with the Scherer formula **equations (7)** [2, 3, 61].

$$D = \frac{0.9\lambda}{\beta \cos\theta} \quad \text{---------- (7)}$$

Where D is the crystalline size of catalysts, λ is the wavelength of the X-ray beam operating system, β is the full-width half maximum calculated from the highest intensity peak and θ is the angle of diffraction.

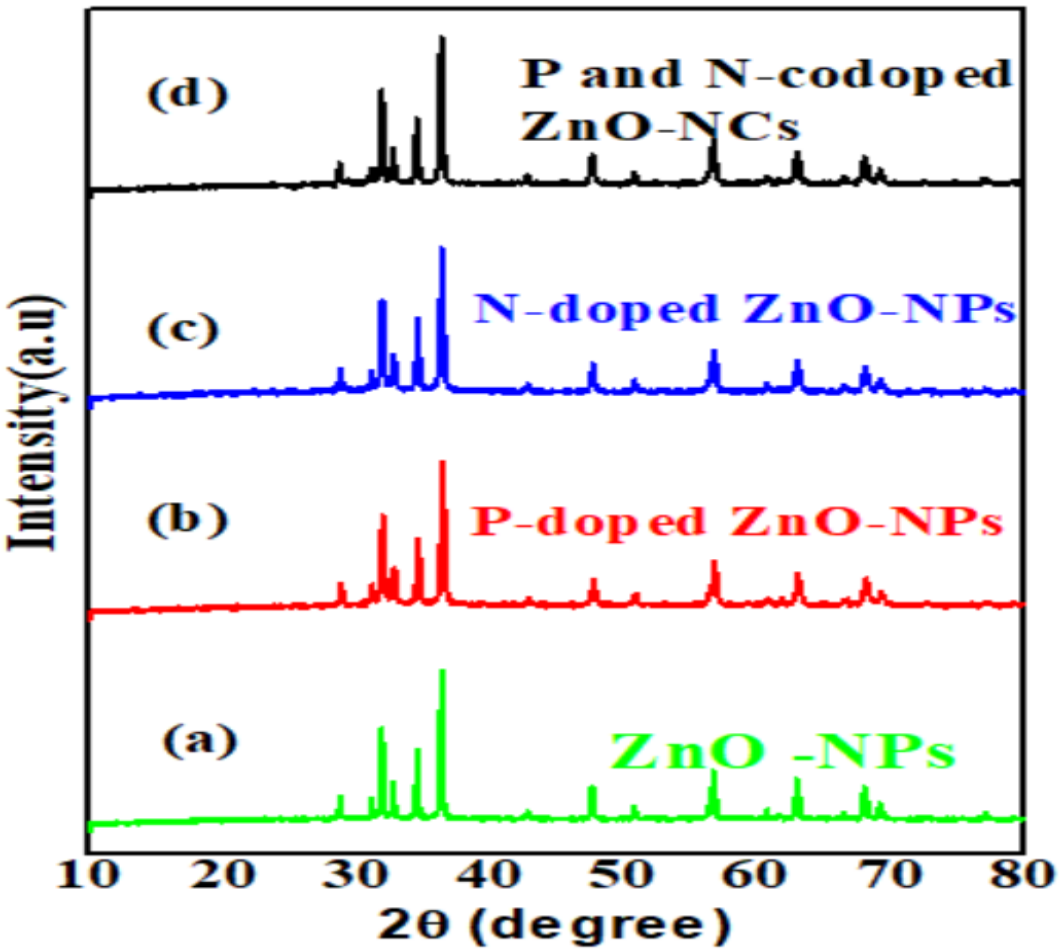

Figure 6. *The XRD Pattern of (a) ZnO-NPs, (b) P-doped ZnO-NPs, (c) N-doped ZnO-NPs and (d) P and N-codoped ZnO-NCs.*

Figure 7 indicates the FTIR spectra evaluations to differentiate the chemical structures of the constituents connected to the surface of ZnO-NPs, P-doped ZnO-NPs, N-doped ZnO-NPs and P & N-codoped ZnO-NCs [62]. The Nanomaterials' FT-IR spectral bands were registered between 4000 and 400 cm^{-1}. The most significant peaks that were identified at 3,460 cm^{-1} represent the C-H stretching vibration and O-H stretching vibration of carboxylic acids and can be the formation of intra- and inter-molecular hydrogen bonds in the sample [63]. The peak at 1,631 cm^{-1} is relevant to carbonyl groups that encounter C=O stretching and perchance acidic carbonyl groups [6]. The sharp peak at around 1,377 cm^{-1} and 1,408 cm^{-1} indicates the existence of the carboxylic acid COO- group. In the vicinity of 1,030 and 807 cm^{-1}, C-O-C stretching becomes visible [3]. The peak around 552 cm^{-1} can be ascribed to the stretching vibration of the Zn-O bond [1, 41]. By analyzing the strong absorption ZnO-NPs peak in the P and N-codoped ZnO-NCs, the intensity

of the ZnO-NPs was slowly decreased in the P and N-codoped ZnO-NCs due to successful capping of Phosphorus and Nitrogen on the surface of Nanoparticles [62]. Most of the signals for different functional groups, as indicated in **Figure 7 (d)** determine that these reducing groups are delegated for creating and stabilizing the synthesis of nanoparticles [65].

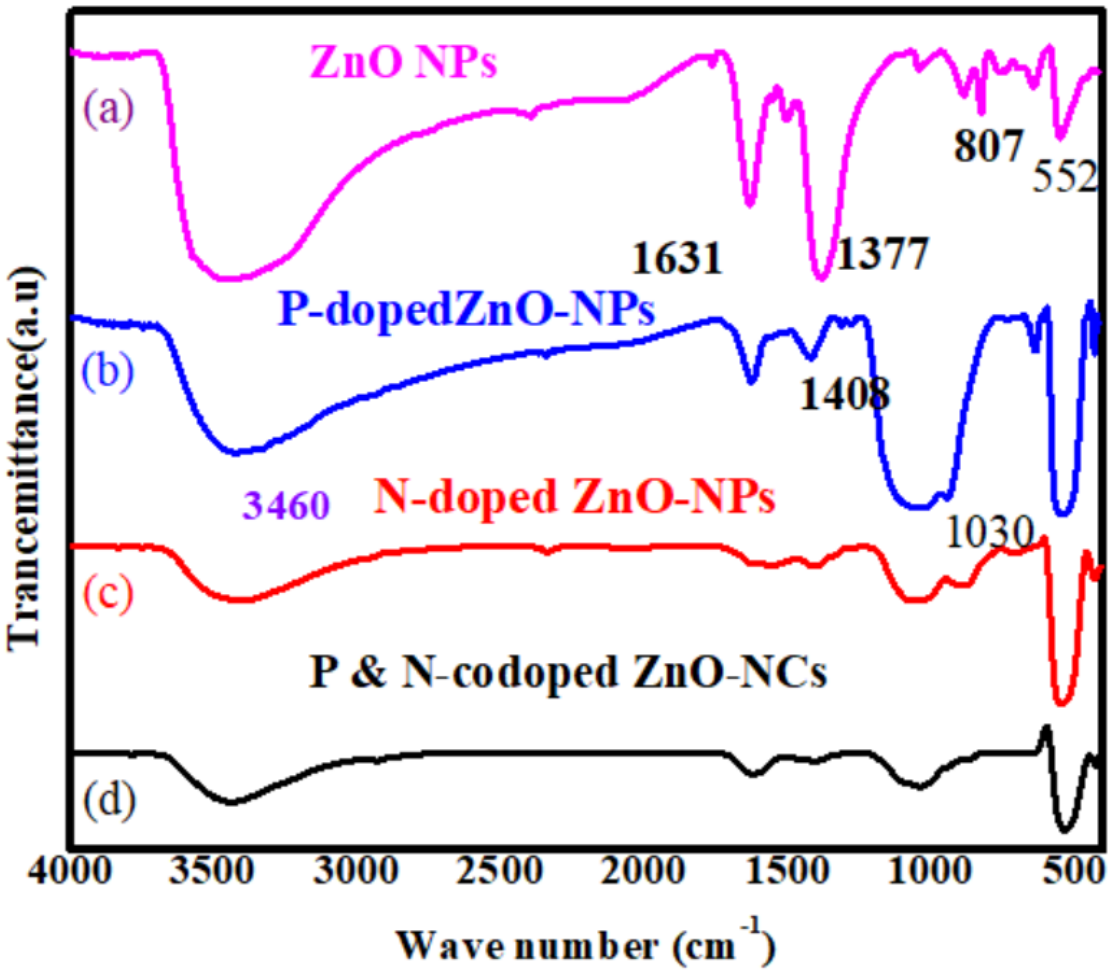

Figure 7.*FT-IR Spectrum of (a) ZnO-NPs, (b) P-doped ZnO- NPs, (c) N-doped ZnO-NPs, and (d) P and N-Codoped ZnO-NCs*

SEM is one of the most useful analyses for examining the surface morphology of the prepared catalysts. The surface configuration of ZnO-NPs, P-doped ZnO-NPs, N-doped ZnO-NPs, and P and N-codoped ZnO-NCs are shown in **Figure 8**. SEM images were used to obtain the correlative morphological determination of the photocatalyst. The SEM images of ZnO-NPs indicated that the surface morphologies are in the form of aggregation and boxy or cubical separation over the whole surface as expressed in **(Figure 8 (b)** and which is strongly similar to

the described according to the recent work and previous variety of literature findings [7]. The photocatalysts surface was improved the cationic dye was preferred to the most relevant to its surface and the photocatalytic effectiveness was enhanced as a consequence of the combination of lower crystalline P-doped ZnO-NPs in **Figure 8 (b**). A diversity of spherical-shaped, rounded, and holey structures was observed in the condition of P and N-codoped ZnO-NCs which nearly corresponds to the stated literature SEM images [6]. As described in **Figure 8 (c)** N-doped ZnO-NPs indicated smaller particle sizes while the ZnO-NPs sample displays relatively larger particle sizes at different enlargements between (3000 and 5000). Nanocomposites have larger particle size scattering arrangements than Nanoparticles. Therefore SEM results obtained, by characterization of ZnO-NPs, P-doped ZnO-NPs, N-doped ZnO-NPs, and P and N-codoped ZnO-NCs which described that P-doped ZnO-NPs **Figure 8(d)** creates agglomerations larger particles sizes.

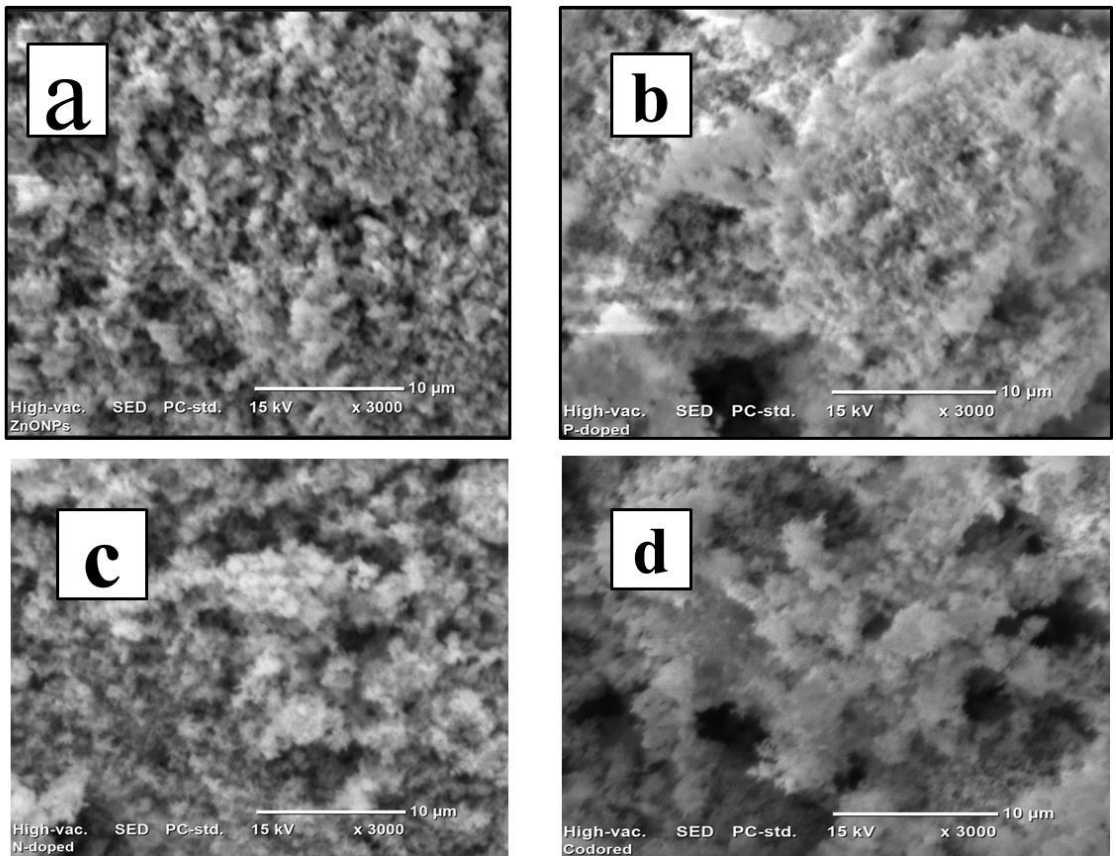

Figure 8. *SEM images of (a) ZnO-NPs, (b) P-doped ZnO- NPs, (c) N-doped ZnO-NPs, and (d) P and N-codoped ZnO-NCs.*

4.2. Photocatalytic Activity

In the recent evaluation, the photocatalytic degradation of the methylene blue (MB) dye was determined by using ZnO-NPs and P and N-codoped ZnO-NCs that were synthesized using ZnO -NPs and exposed to sun radiation in Jimma University at intervals of 10, 30, 40, 50, 60, 70 and 80 minutes. The distinguishable MB absorption peak strength was obtained at 665 nm and steadily decreased after the dye degradation was usually differentiated by gradually changing the dye solutions from blue color to colorless [66, 67].

4.3. Optimization of Photocatalytic Degradation of Methylene Blue (MB) Dye

Generally, photocatalytic degradation was carried out by using catalyst dose, point zero charge, effect of pH, the effect of initial dye concentration, and effect of contact time, which were considered before the true photocatalytic test was carried out, as seen in **Figure 9** [13].

4.4. Effect of catalyst dosage

One of the most important points necessary for the degrading result of pollutants is the quantity of the photocatalyst. It is necessary to determine the ideal photocatalyst dose for effective dye removal to protect using a very small quantity. As a consequence several experiments were carried out to examine the ideal concentration of photocatalyst P and N-codoped ZnO-NCs by using its amount to 15, 25, and 35 mg/L in the initial concentration of MB dye 50 mL as the quantity of catalyst is changed the degree of MB dye degradation efficiency is depicted as **Figure 9 (a)** [69]. Far, it is necessary to note that the NCs have high absorption sites and a larger surface area when exposed to sunlight for the manufacturing of hydroxyl free radicals. The free radicals also have a higher option of contacting with MB dye pollutants. As the catalyst dosage was increased, the removal of MB percentage removal was decreased [69]. The increased cloudiness of the suspension screens the photocatalytic process and decreases light penetration. According to **Figure 9,** the degradation of MB rose from 36 % to 97 % when the dosage of P and N-codoped ZnO-NCs increased from 10 mg to 30 mg. MB degradation did not increase with the dosage increases after 30 mg yet [27]. Consequently, the catalyst dosage of 30 mg was obtained to be ideal for the photocatalytic degradation of 50 mL MB.

4.5. Point Zero Charge

Point zero charge (PZC) is earned when the overall total particles are zero at a specific pH value [70]. Throughout photocatalysis, the PZC of NCs is an essential criterion to evidence the arbitrary charge surface of photocatalysts. This occupation occurred in the PZC of the P and N-cooped ZnO-NCs in the pH ranges 6, 8, and 9 [65]. During the pH of the solution is greater than the PZC value, the composite preference the photolysis of positively charged particles while as the pH value becomes smaller than the PZC, the nanocomposite preference for adsorption of negatively charged dyes is pollutants [65, 70]. Dominating the pH of the photocatalytic system can shape the surface charge of the photocatalyst, supplying the capability for particular degradation of particular dyes. For this reason, MB is a familiar cationic dye, and a pH value higher than the PZC is preferable for its decomposition **Figure 9 (b)** [65].

4.6. Effect of pH Values

Dye's degradation and adsorption are based on the pH value of the intermediate. The speed of degradation in the photocatalytic method is based on the pH positions and the adsorption tendency of the dyes on the photocatalyst. An enlargement in the number of desired molecules adsorbed on the catalyst results in a greater molecular degradation speed [69]. To deal with the effect of the pH on the performance of MB degradation and adsorption tendency, the pH of the MB solution was used 6, 8, and 9 by adjusting 0.1M NaOH and HCl solutions. The catalyst dosage was 20 mg and 10 mg/L dye was used for 80 minutes **Figure 9 (d)** indicates the scheme percentage degradation at various pH values. It can be examined from the schematic of the photocatalytic activity of MB dye on P and N-codoped ZnO-NCs elevated with pH up to 8. The higher degradation inadequacy was accomplished at pH 8 which is relatively the PZC value of the solution [71]. At acidic pH interrelation of H^+ ion and cation MB as well as the repulsive force attraction between the dye cation and the positive charge sites, resulted in low MB dye removal. However inversely, at higher pH hydroxyl groups from the base caused the formation of metal hydroxide complexes, which indicates to decrease in MB dye removal. This result was limited to the effect of prepared nanocatlysts and decreased the production of free radicals, on the surface of photocatalyst under sunlight radiation. Thus at 8 0minutes the higher removal of MB dye was 97 % when P and N-codoped ZnO-NCs was added at pH of 8 [69].

4.7. Effect of initial Dye concentrations

Differing the initial dye concentration (10 to 30 mg/L) to determine the optimal dose. NCs indicate higher photocatalytic at a low dye concentration of 10 mg/L but decreased efficiency at a high dye concentration. **Figure 9 (d)**. Due to this reason when the concentration of dye increases the solution's color becomes more intense, and the photons reach the surface, reducing the production of hydroxyl radicals [72]. As a consequence only a small amount of photon reach the catalytic surface, reducing the production of hydroxyl radicals. The formation of hydroxyl radicals on the catalyst' surface is possibly to decrease since the dye ion produces an active site on the surface catalyst's surface. With increasing concentration, the degradation efficiency of MB dye ion decreases, with the high efficiency of 97 % found at 10 mg/L of MB concentration when P and N-cooped ZnO-NCs were added at a pH of 8. The photodegradation efficiency of 10 mg/L, 20 mg/L, and 30 mg/L MB dye at the end of 80 minutes was 97 %, 91 %, and 36 % respectively. A schematic representation of the mechanism of dye decomposition is given in **Figure 9** [13].

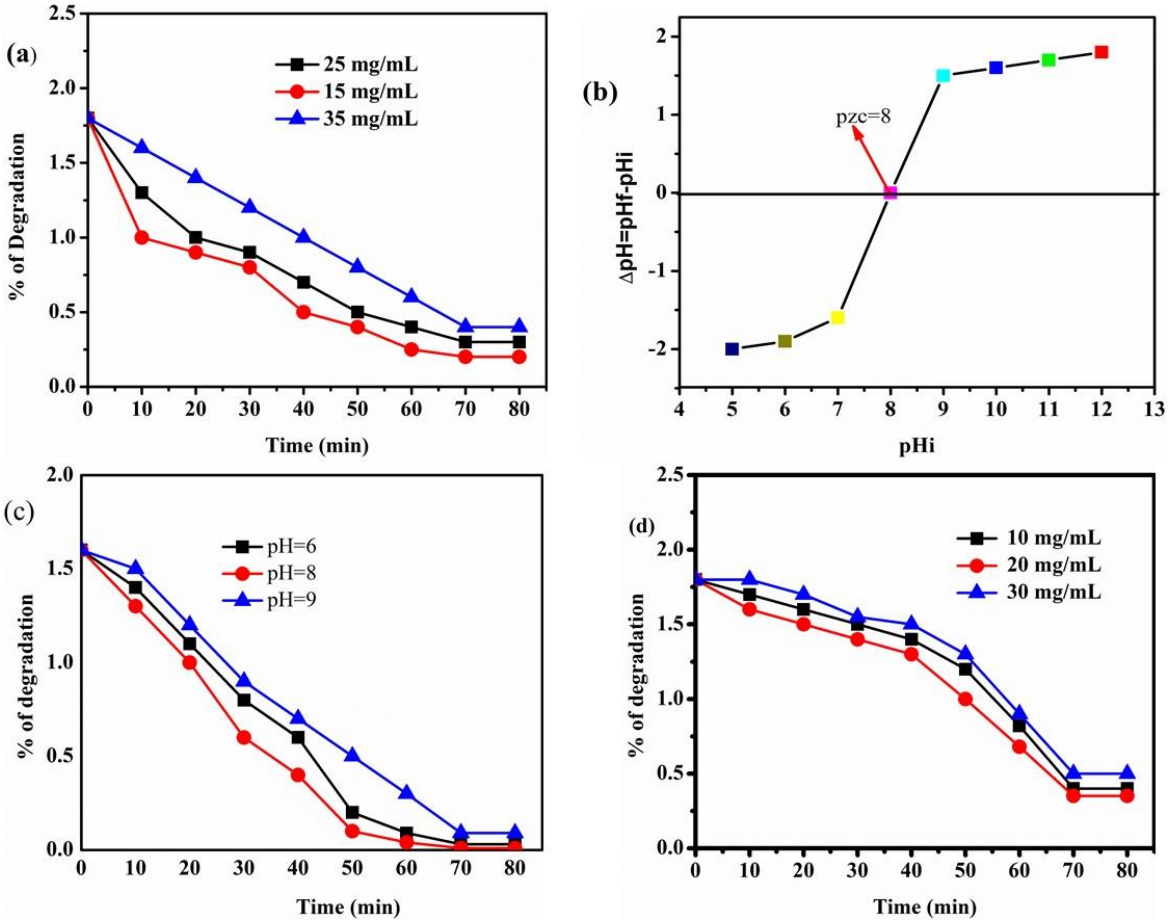

Figure 9*. Degradation Efficiency of MB on the Different Parameters A) Dosage of Catalyst B) Point Zero Charge C) pH Value of Solution D) Initial Concentration of MB.*

4.8. Effect of contact time

Prepared ZnO-NPs and P and N-codoped ZnO-NCs their photocatalytic properties were obtained by decomposition of MB dye. UV-Vis absorbance was obtained to indicate the impact of irradiation time on the degradation of MB dye and the degradation percentage was determined by measuring the absorbance. A sample of 20 mg/L dye at pH 8 was taken in a volumetric flask and 50 mg of the photocatalyst was added and exposed to light with continuous stirring for 10, 20, 30, 40, 50,60, 70, and 80 minutes [4]. After stirring, the light was irradiated to three separate systems; pure MB, ZnO- NPs containing MB and P, and N-codoped ZnO-NCs, and their UV-Vis absorption spectrum was determined after every 10 minutes **Figure 10 (a)** indicates the UV-Vis absorption spectrum of the degradation kinetics of MB. For the MB containing pure ZnO-NPs the absorbance peaks were progressively decreased up on light irradiation **Figure 10(a).** From

the UV-Vis characterization, the peak intensity of the MB sample containing N and P-doped ZnO-NCs dramatically decreased upon becoming almost Zero after 80 minutes of light irradiation **Figure 10 (b).** Following the absorbance peak intensity decreases the color of the solution also faded and became colorless after 80 minutes of irradiation **Figure 10 (d) (i-iii).** The maximum degradation efficiency of MB dye was attained by Uncatalyzed, pure ZnO-NPs catalyzed and NCs were 36 %, 91 %, and 97 % respectively MB was degraded within 80 minutes of contact time. On the contrary, MB without the catalyst resisted light degradation, and peak intensities were almost retained after 80 minutes of light irradiation [70]. The absence of obvious degradation of MB without the photocatalysts (blank test) under light irradiation shows that the contribution of self-degradation of MB is significant and that it resists photodegradation. The slight degradation of MB in pure ZnO-NPs is also attributed to the slow photocatalytic behavior of ZnO-NPs in visible light due to its high energy band gap. To improve the photocatalytic behavior of ZnO-NPs, doping or forming NCs is very necessary to shift the energy band gap towards the red. Incorporation of P-doped and N-doped ZnO-NPs into pure ZnO-NPs enhances the surface charge and surface area and shifts the band gap to the red **Figure 10 (d) (ii)** boosting photocatalytic behavior. As a result, MB with P and N-codoped ZnO-NCs degrades and the blue color disappears in an hour **Figure 10 (d) (ii).**

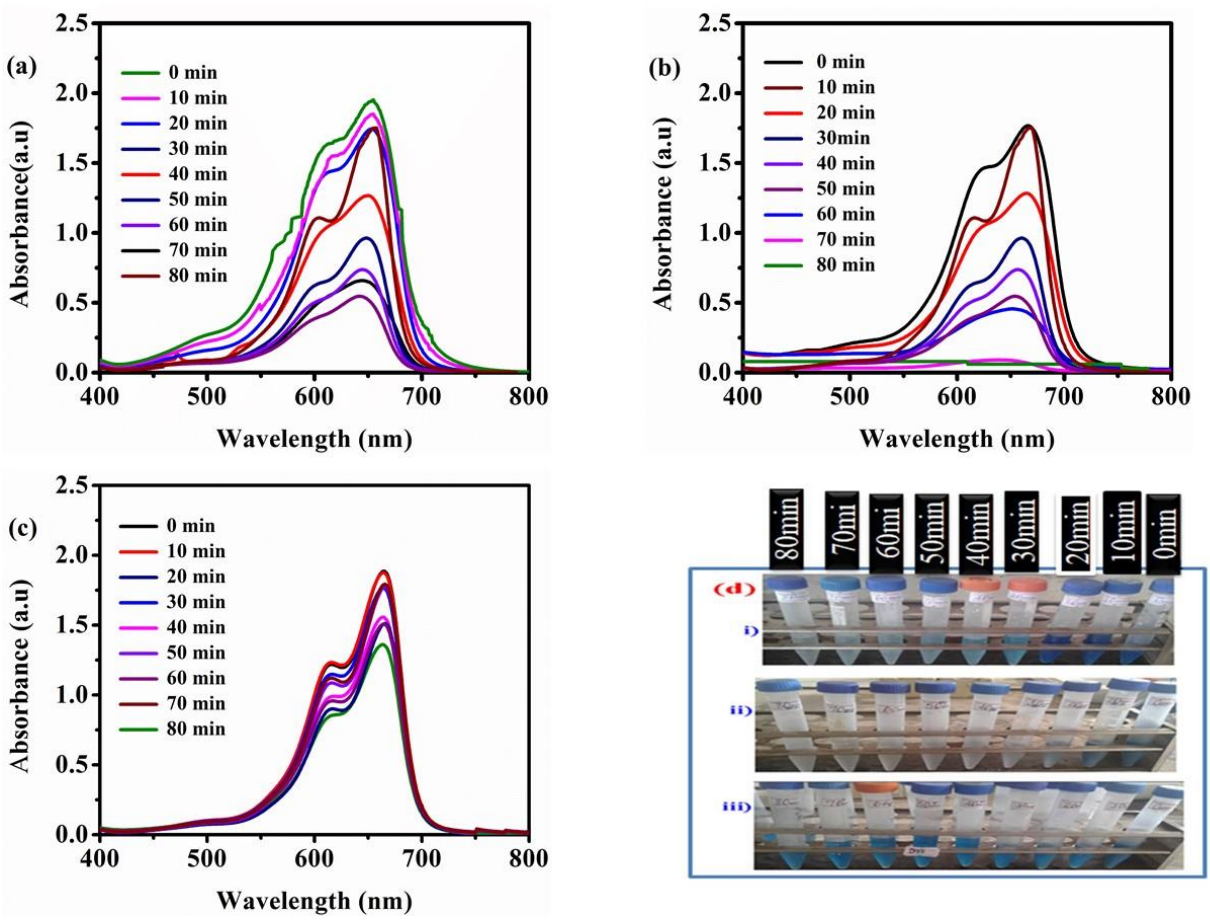

Figure 10*. (a-c) shows UV-Vis absorption spectrum for degradation kinetics of MB on (a)in the presence ZnO-NPs (b) in the presence of P and N-codoped ZnO-NCs (c) photocatalysis under sunlight irradiation (d) pictures MB at different removal stages with (i) ZnO-NPs (ii) P and N-codoped ZnO-NCs (iii) as the catalyst and without catalysts.*

Figure 11 shows the reusability of P and N-codoped ZnO-NCs' for dye decomposition was evaluated by the 3-cycle degradation of MB dye. The photocatalyst was rinsed with ethanol after each cycle and reused. The repetitions of the P and N-codoped ZnO-NCs photocatalyst can be recycled. Using similar optimal operating parameters as the P and N-codoped ZnO-NCs, we produced the reusability test. For the first three cycles, degradation effectiveness was 97 %, 91.5 %, and 87 % respectively at an initial dye concentration of 50 mg, catalyst dose of 15 mg, pH of 8, and 80 minutes irradiation time. The photocatalytic degradation effectiveness of P and N-codoped ZnO-NCs decreases in the second and third cycles, which may be due to the aggregations of waste ions and catalyst dosage indicating impurities. These experiments verify that the prepared P and N-codoped ZnO-NCs photocatalyst can be recycled for three successive

cycles with a moderate decrease in efficiency. Thus, P and N-codoped ZnO-NCs were completed as a stable and effective photocatalyst.

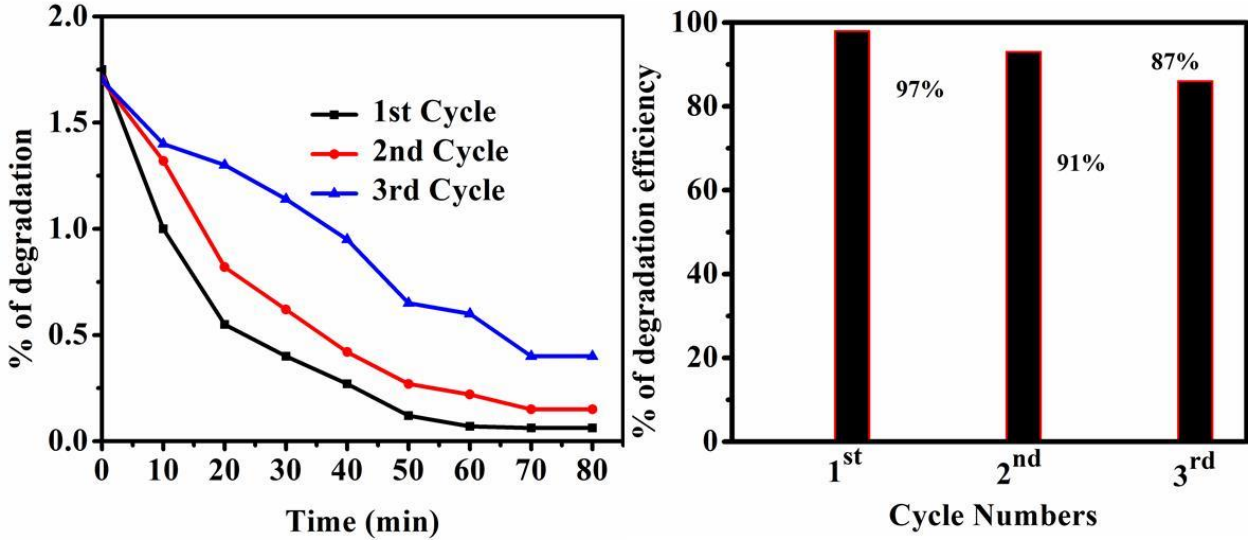

Figure 11*. Recyclability of P and N-codoped ZnO-NCs using identical optimal operating parameters as we performed for the P and N-codoped ZnO-NCs in this experimental work, an initial dye concentration of 50 mg, a catalyst dose of 15 mg, at a pH of 8, and 80 minutes irradiation time.*

Radical scavenging activity is concerned with developing processes, disinfections, drug delivery, and cancer therapy [45]. Consequently, in the recent investigation the DPPH radical scavenging activity of a biological product that possesses biological properties. The tendency of scavenging DPPH radical was measured by **Equation (6)** [40,72].

The prepared ZnO-NPs and P and N-codoped ZnO-NCs were examined for anti-oxidant properties using DPPH radical scavenging investigated. The tendency to scavenge the DPPH radical was increased as the concentration of examined samples increased from 5–80 µg/mL indicated in **Figure 12** [10]. The DPPH radical scavenging activity of ZnO-NPs and P and N-codoped ZnO-NCs and Ascorbic acid at half-maximal inhibition concentration (IC_{50}) was found in the respective orders of Ascorbic acid > ZnO-NPs, 80 µg/mL > ZnO-NPs, 40 µg/mL > ZnO-NPs, 20 µg/mL > ZnO-NPs,10 µg/mL and ZnO-NPs, 5 µg/mL. The DPPH radical scavenging activity methods of P and N-codoped ZnO-NCs examined and ascorbic acid at 80 µg/mL are in the ordered of Ascorbic acid > P and N-codoped ZnO-NCs, 80 µg/mL > P and N-codoped ZnO-NCs, 40 µg/mL> P and N-codoped ZnO-NCs, 20 µg/mL > P and N-codoped ZnO-NCs, 10 µg/mL > P and N-codoped ZnO-NCs, 5 µg/mL depending on the reduction of DPPH, a stable

free radical [39]. This result indicates that P and N-codoped ZnO-NCs can protect against oxidation by transferring electron density from oxygen to carbon in DPPH free radical through n→π* transition [6].

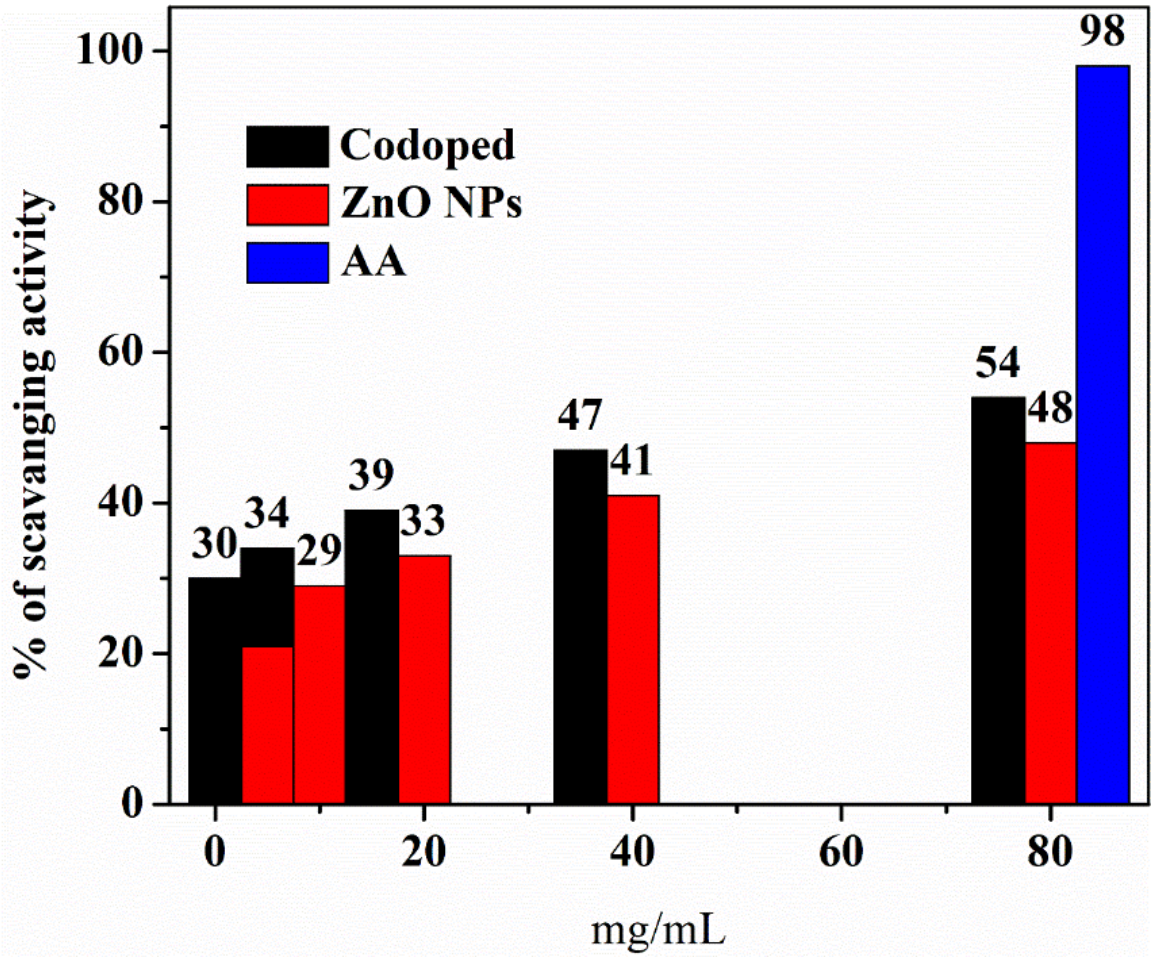

Figure 12*. The radical scavenging activities of ZnO -NPs, P and N- codoped ZnO- NCs and AA*

4.9. Antimicrobial activity

To examine the antimicrobial activity of ZnO-NPs, P-doped ZnO-NPs, N-doped ZnO-NPs, and its P and N-cooped ZnO-NCs the disk diffusion method was used against gram-negative and gram-positive bacterial strains. DMSO was used as gram negative control while Gentamicin was used as a positive control [73]. The antibacterial activities of 25 mg/mL, 50 mg/mL, and 75 mg/mL, of prepared NPs were examined against, S. aureus, E.coli, B.cereus, and S.typhi **Figure 13** [10, 36]. The consequence of the study signifies that gram-positive bacteria, such as E.col and B.cerus were more affected by the synthesized of ZnO-NPs, P-doped ZnO-NPs, N-doped

ZnO-NPs and its P and N-codoped ZnO–NCs than strains like S.typhi and S.aureus [48]. Furthermore, the zinc ions (Zn^{+2}) released from NPs could tie to the negatively charged bacterial cell wall, creating cleavage, and leading to protein denaturation and cell death [31]. Small-sized nanoparticles (NPs) have a high penetration tendency and influence rapid cell death. Small-sized NPs have a high penetration tendency and influence rapid cell harm compared to the other bulky compounds. As NP concentration increases antimicrobial activity upgrades, components with the indicated literature [42]. The NCs' antimicrobial activity is preparable to that of ZnO-NPs, P-doped ZnO-NPs, and N-doped ZnO-NPs leading that combination of ZnO-NPs to better advance the NCs' antimicrobial activity. The inhibition zone of antimicrobial measurements is expressed in **Table 1** [41].

Table 1. Microbial activity of ZnO-NPs, N-doped ZnO NPs, P-doped ZnO NPs, and its P and N-codoped ZnO nanocomposites.

Microorganism	**Inhibition zone (mm)**					
	Control		**Target Materials (75 mg/mL)**			
	DMSO (-ve)	Gentamicin (+ve)	ZnO NPs	N doped ZnO NPs	P doped ZnO NPs	P & N-cooped ZnO-NCs
S.aureus	0	23	10	12	12	15
B.ceraus	0	25	12	13	13	15
E.coli	0	24	10	10	16	18
S.typhi	0	25	11	13	12	14
C.al	0	17	11	15	12	16

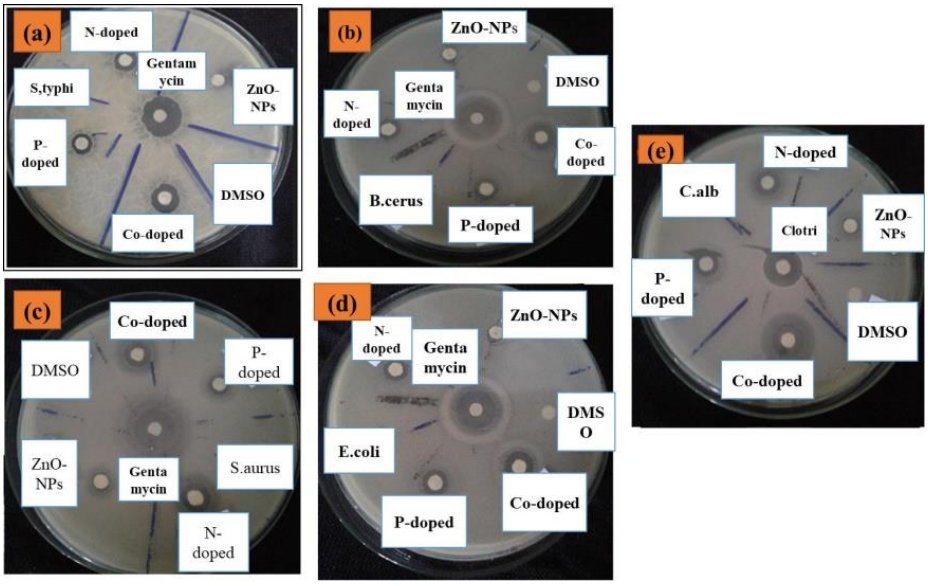

Figure 13*. Antimicrobial activity of ZnO-NPs, P-doped ZnO-NPs, N-doped ZnO-NPs and its P and N- codoped ZnO- NCs of (a) S.typh (b) B.Cer (c) S.aur (d) E.Coli (e) C.alb Respectively.*

5.Conclusion

ZnO nanoparticles and their P and N-codoped ZnO-nanocomposites were prepared using the sol-gel method with aqueous forerunner solutions. We determined the crystal structure, band gap energy, bond vibration properties, and morphologies of the photocatalysts using UV–Vis, FT-IR, XRD, and SEM. As a result, the incorporation of P-doped ZnO-NPs and N-doped ZnO-NPs to ZnO-NPs determines surface charge and similarity, as indicated by FTIR analysis. This also led to a reduction in the energy band gap of ZnO-NPs from 2.92 to 2.53 eV. The prepared nanoparticles and nanocomposite treated with MB dyes were under visible light to evaluate their photocatalytic activity. As a result, MB dye was successfully decolorized by the P and N-codoped ZnO-NCs photocatalyst under direct solar irradiation was examined from pH PZC and FT-IR measurements that the addition of P-doped ZnO-NPs and N-doped ZnO-NPs to ZnO-NPs materials enhanced the surface charges of the nanocomposites, resulting in refined photocatalytic degradation efficiency. Due to the improved surface charge, the photocatalytic degradation efficiency of P and N-codoped ZnO-NCs exceeds that of pure ZnO-NPs. P and N-codoped ZnO-NCs prepared at pH 8 achieved an optimum efficiency of 97 % degradation of MB dye. The importance of band gap reduction, high photocatalytic performance, and excellent antimicrobial

activity and antioxidant of the P and N-codoped ZnO-NCs compared with ZnO-NPs. This approach can enhance the photocatalytic properties of various nano photocatalysts. The photocatalytic degradation effectiveness in the reusability of P and N-codoped ZnO-NCs reduced in the order of 97 %, 91.5 %, and 87 % respectively in the first, second, and third cycles may be due to the collection of waste ions and catalyst dosage indicating impurities.

5.1 Recommendation

During a research study, researchers observed different uses of the researcher that are relevant for future research. The study involved characterizing ZnO-NPs and NCs using EDS, TEM, and XPS techniques. EDS is a powerful technique that enables the operator to determine the chemical composition of a sample more accurately and rapidly than SEM. TEM generates higher-resolution images, provides atomic and crystallographic data, produces 2D images that are easier to interpret than 3D SEM images, and allows users to examine more of a given sample. On the other hand, XPS provides detailed information about the surface composition and chemical states, while SEM offers high-resolution imaging of surface morphology and topology. The study also found that ZnO-NCs can be used for photocatalytic degradation of harmful dyes, such as Methyl Orange and Rhodamine B. These dyes have been shown to have carcinogenic, mutagenic, and teratogenic effects on humans and animals, making it important to find effective ways to remove them from the environment.

6. REFERENCES

[1] Salari, P.; Moghaddam, M. G.; Bahreini, M.; Reza, M. Green Synthesis of ZnO Nanoparticles from Foeniculum Vulgare Mill. Seed Extract and Its Antibacterial Effects on Foodborne Bacteria. **2023**, *22* (3), 14–26.

[2] Abel, S.; Tesfaye, J. L.; Shanmugam, R.; Dwarampudi, L. P.; Lamessa, G.; Nagaprasad, N.; Benti, M.; Krishnaraj, R. Green Synthesis and Characterizations of Zinc Oxide (ZnO) Nanoparticles Using Aqueous Leaf Extracts of Coffee (Coffea Arabica) and Its Application in Environmental Toxicity Reduction. **2021**, *2021*.

[3] Ghdeeb, N. J.; Hussain, N. A. Nano Biomed Eng Antimicrobial Activity of ZnO Nanoparticles Prepared Using a Green Synthesis Approach. **2023**, *15* (1), 14–20.

[4] Faisal, S.; Jan, H.; Shah, S. A.; Shah, S.; Khan, A.; Akbar, M. T.; Rizwan, M.; Jan, F.; Akhtar, N.; Khattak, A.; et al. Green Synthesis of Zinc Oxide (ZnO) Nanoparticles Using Aqueous Fruit Extracts of Myristica Fragrans : Their Characterizations and Biological and Environmental Applications. **2021**. https://doi.org/10.1021/acsomega.1c00310.

[5] Yilma, T.; Kassaw, M.; Murthy, H. C. A.; Dekebo, A. ZnO Nanoparticles Synthesized Using Aerial Extract of Ranunculus Multi Fi Dus Plant : Antibacterial and Antioxidant Activity. **2023**, *2023*.

[6] Fabbiyola, S.; Kennedy, L. J.; Aruldoss, U.; Bououdina, M.; Dakhel, A. A.; Judithvijaya, J. Synthesis of Co-Doped ZnO Nanoparticles via Co-Precipitation : Structural, Optical and Magnetic Properties. *Powder Technol.*, **2015**, *286*, 757–765. https://doi.org/10.1016/j.powtec.2015.08.054.

[7] Sharma, N.; Kumar, S. Role of Method of Preparation for Co-Doping in Structural and Optical Properties of Ag-Doped Zno Nanoparticles. *Int. J. Chem. Phys. Sci.*, **2018**, *7* (1), 18. https://doi.org/10.30731/ijcps.7.1.2018.18-25.

[8] Lavand, A. B.; Malghe, Y. S. Synthesis, Characterization and Visible Light Photocatalytic Activity of Nitrogen-Doped Zinc Oxide Nanospheres. *J. Asian Ceram. Soc.*, **2015**, *3* (3), 305–310. https://doi.org/10.1016/j.jascer.2015.06.002.

[9] Elias, M.; Uddin, M. N.; Saha, J. K.; Hossain, M. A.; Sarker, D. R.; Akter, S.; Siddiquey, I. A.; Uddin, J. A Highly Efficient and Stable Photocatalyst; N-Doped ZnO/CNT Composite Thin Film Synthesized via Simple Sol-Gel Drop Coating Method. *Molecules*,

2021, *26* (5). https://doi.org/10.3390/molecules26051470.

[10] Odoi, M.; Kwabena, E.; Ayertey, F.; Naana, G.; Archer, M.; Kumadoh, D.; Oteng, S.; Kwesi, P.; Ampomah, A. Synthesis and Characterization of ZnO Nanomaterial from Cassia Sieberiana and Determination of Its Anti-Inflammatory, Antioxidant and Antimicrobial Activities. *Sci. African*, **2023**, *19*, e01452. https://doi.org/10.1016/j.sciaf.2022.e01452.

[11] Kalpana, S.; Krishnan, S. S.; Senthil, T. S.; Elangovan, S. V. COBALT DOPED ZINC OXIDE NANOPARTICLES FOR PHOTOCATALYTIC APPLICATIONS. **2017**, *13* (5), 263–269.

[12] Chauhan, N.; Singh, V.; Kumar, S.; Kumari, M.; Sirohi, K. Preparation of Silver and Nitrogen Co-Doped Mesoporous Zinc Oxide Nanoparticles by Evaporation Induced Self Assembly Process to Study Their Photocatalytic Activity. *J. Sol-Gel Sci. Technol.*, **2019**. https://doi.org/10.1007/s10971-019-04969-6.

[13] Sharma, S. S.; Palaty, S.; John, A. K. Band Gap Modified Zinc Oxide Nanoparticles: An Efficient Visible Light Active Catalyst for Wastewater Treatment. *Int. J. Environ. Sci. Technol.*, **2021**, *18* (9), 2619–2632. https://doi.org/10.1007/s13762-020-02976-7.

[14] Sharma, A.; Khangarot, R. K.; Kumar, N.; Chattopadhyay, S.; Misra, K. P. Rise in UV and Blue Emission and Reduction of Surface Roughness Due to the Presence of Ag and Al in Monocrystalline ZnO Films Grown by Sol-Gel Spin Coating. *Mater. Technol.*, **2021**, *36* (9), 541–551. https://doi.org/10.1080/10667857.2020.1776029.

[15] Kumari, M.; Kundu, V. S.; Kumar, S.; Swatch, S.; Chauhan, N. Nitrogen and Silver Codoped One-Dimensional ZnO Nanostructure for Optoelectronic Application. *J. Sol-Gel Sci. Technol.*, **2020**, *93* (2), 302–308. https://doi.org/10.1007/s10971-019-05129-6.

[16] Lu, J.; Zhu, J.; Wang, Z.; Cao, J.; Zhou, X. Rapid Synthesis and Thermal Catalytic Performance of N-Doped ZnO/Ag Nanocomposites. *Ceram. Int.*, **2014**, *40* (1 PART B), 1489–1494. https://doi.org/10.1016/j.ceramint.2013.07.033.

[17] Baruah, S.; Najam, M.; Joydeep, K. Perspectives and Applications of Nanotechnology in Water Treatment. *Environ. Chem. Lett.*, **2016**, *14* (1), 1–14. https://doi.org/10.1007/s10311-015-0542-2.

[18] Yusuf, A.; Al Jitan, S.; Garlisi, C.; Palmisano, G. A Review of Recent and Emerging Antimicrobial Nanomaterials in Wastewater Treatment Applications. *Chemosphere*, **2021**,

278. https://doi.org/10.1016/j.chemosphere.2021.130440.

[19] Biswas, P.; Ahmed, S.; Dey, D.; Kaium, A.; Rafi, A.; Yasmin, F.; Kumar, S.; Islam, A.; Ishraq, T.; Abdullah, A.; et al. Biomedicine & Pharmacotherapy Advanced Implications of Nanotechnology in Disease Control and Environmental Perspectives. *Biomed. Pharmacother.*, **2023**, *158*, 114172. https://doi.org/10.1016/j.biopha.2022.114172.

[20] P.U., I.; C.C., C.; F.C., I.; I.F., F.; C.A., O. A Review of Environmental Effects of Surface Water Pollution. *Int. J. Adv. Eng. Res. Sci.*, **2017**, *4* (12), 128–137. https://doi.org/10.22161/ijaers.4.12.21.

[21] Shah, J. H.; Fiaz, M.; Athar, M.; Ali, J.; Rubab, M.; Mehmood, R.; Jamil, S. U. U.; Djellabi, R. Facile Synthesis of N/B-Double-Doped Mn2O3 and WO3 Nanoparticles for Dye Degradation under Visible Light. *Environ. Technol. (United Kingdom)*, **2020**, *41* (18), 2372–2381. https://doi.org/10.1080/09593330.2019.1567604.

[22] Dadkhah, M.; Tulliani, J. M. Green Synthesis of Metal Oxides Semiconductors for Gas Sensing Applications. **2022**.

[23] Asghar, F.; Mushtaq, A. The Future of Nanomaterial in Wastewater Treatment : A Review. **2023**, *23* (1), 150–157.

[24] Boulahlib, S.; Dib, K.; Özacar, M.; Bessekhouad, Y. Optical, Dielectric, and Transport Properties of Ag-Doped ZnO Prepared by Aloe Vera Assisted Method. *Opt. Mater. (Amst).*, **2021**, *113* (February). https://doi.org/10.1016/j.optmat.2021.110889.

[25] Mun, K.; Wei, C.; Sing, K.; Ching, J. Recent Developments of Zinc Oxide Based Photocatalyst in Water Treatment Technology : A Review. *Water Res.*, **2016**, *88*, 428–448. https://doi.org/10.1016/j.watres.2015.09.045.

[26] Huang, L.; Zang, W.; Ma, Y.; Zhu, C.; Cai, D.; Chen, H.; Zhang, J.; Yu, H.; Zou, Q.; Wu, L.; et al. In-situ Formation of Isolated Iron Sites Coordinated on Nitrogen-Doped Carbon Coated Carbon Cloth as Self-Supporting Electrode for Flexible Aluminum-Air Battery. *Chem. Eng. J.*, **2021**, *421* (January). https://doi.org/10.1016/j.cej.2021.129973.

[27] Chauhan, N.; Singh, V.; Kumar, S.; Sirohi, K.; Swatch, S. Synthesis of Nitrogen- and Cobalt-Doped Rod-like Mesoporous ZnO Nanostructures to Study Their Photocatalytic Activity. *J. Sol-Gel Sci. Technol.*, **2019**, *91* (3), 567–577. https://doi.org/10.1007/s10971-019-05059-3.

[28] Saadi, H.; Benzarti, Z.; Rhouma, F. I. H.; Sanguino, P.; Guermazi, S.; Khirouni, K.

Enhancing the Electrical and Dielectric Properties of ZnO Nanoparticles through Fe Doping for Electric Storage Applications. *J. Mater. Sci. Mater. Electron.*, **2021**, *32* (2), 1536–1556. https://doi.org/10.1007/s10854-020-04923-1.

[29] Saini, D.; Aggarwal, R.; Sonker, A. K.; Sonkar, S. K. Photodegradation of Azo Dyes in Sunlight Promoted by Nitrogen-Sulfur-Phosphorus Codoped Carbon Dots. *ACS Appl. Nano Mater.*, **2021**, *4* (9), 9303–9312. https://doi.org/10.1021/acsanm.1c01810.

[30] Nadeem, M. S.; Munawar, T.; Mukhtar, F.; Naveed, M.; Riaz, M.; Iqbal, F. Enhancement in the Photocatalytic and Antimicrobial Properties of ZnO Nanoparticles by Structural Variations and Energy Bandgap Tuning through Fe and Co Co-Doping. *Ceram. Int.*, **2021**, *47* (8), 11109–11121. https://doi.org/10.1016/j.ceramint.2020.12.234.

[31] Akbar, N.; Aslam, Z.; Siddiqui, R.; Shah, M. R.; Khan, N. A. Zinc Oxide Nanoparticles Conjugated with Clinically - Approved Medicines as Potential Antibacterial Molecules. *AMB Express*, **2021**, 1–16. https://doi.org/10.1186/s13568-021-01261-1.

[32] Ganesh, I. Al and Li Co-Doping Effects on Structural, Band-Gap, and Photocatalytic Properties of Pyro-Hydrolyzed ZnO Nano-Powder. *Ceram. Int.*, **2016**, *42* (8), 10410–10421. https://doi.org/10.1016/j.ceramint.2016.03.183.

[33] Welderfael, T.; Yadav, O. P.; Taddesse, A. M.; Kaushal, J. Synthesis, Characterization and Photocatalytic Activities of Ag-N-Codoped ZnO Nanoparticles for Degradation of Methyl Red. *Bull. Chem. Soc. Ethiop.*, **2013**, *27* (2), 221–232. https://doi.org/10.4314/bcse.v27i2.7.

[34] Xie, Y.; He, Y.; Irwin, P. L.; Jin, T.; Shi, X. Antibacterial Activity and Mechanism of Action of Zinc Oxide Nanoparticles against Campylobacter Jejuni □. **2011**, *77* (7), 2325–2331. https://doi.org/10.1128/AEM.02149-10.

[35] Mendes, C. R.; Dilarri, G.; Forsan, C. F.; Moraes, V. De; Sapata, R.; Renato, P.; Lopes, M.; Moraes, P. B. De; Montagnolli, R. N.; Ferreira, H.; et al. Antibacterial Action and Target Mechanisms of Zinc Oxide Nanoparticles against Bacterial Pathogens. *Sci. Rep.*, **2022**, 1–10. https://doi.org/10.1038/s41598-022-06657-y.

[36] Hashem, A. H.; Rizk, S. H.; Abdel-Masoud, M. A.; Al-, W. H. RSC Advances Antioxidant Activities of Novel Synthesized Bimetallic Boron Oxide – Zinc Oxide Nanoparticles †. **2023**, 20856–20867. https://doi.org/10.1039/d3ra03413e.

[37] Pascariu, P.; Gherasim, C.; Airinei, A. Metal Oxide Nanostructures (MONs) as

Photocatalysts for Ciprofloxacin Degradation. **2023**.

[38] Welderfael, T.; Pattabi, M.; Pattabi, R. M.; Arun Kumar Thilipan, G. Photocatalytic Activity of Ag-N Co-Doped ZnO Nanorods under Visible and Solar Light Irradiations for MB Degradation. *J. Water Process Eng.*, **2016**, *14*, 117–123. https://doi.org/10.1016/j.jwpe.2016.11.001.

[39] Geremew, A.; Carson, L.; Woldesenbet, S.; Wang, H.; Reeves, S.; Jr, N. B.; Saganti, P.; Weerasooriya, A.; Peace, E. Effect of Zinc Oxide Nanoparticles Synthesized from Carya Illinoinensis Leaf Extract on Growth and Antioxidant Properties of Mustard (Brassica Juncea). **2023**, No. January, 1–16. https://doi.org/10.3389/fpls.2023.1108186.

[40] D, D. A. P.; Plashintania, D. R.; Putri, R. M.; Wibowo, I.; Id, Y. R.; Id, S. H.; Id, A. I. Synthesis of Zinc Oxide Nanoparticles Using Methanol Propolis Extract (Pro-ZnO NPs) as Antidiabetic and Antioxidant. **2023**, 1–18. https://doi.org/10.1371/journal.pone.0289125.

[41] Arif, H.; Qayyum, S.; Akhtar, W.; Fatima, I.; Kayani, W. K.; Rahman, K. U.; Kamal, A.; Ali, S. Synthesis and Characterization of Zinc Oxide Nanoparticles at Different PH Values from Clinopodium Vulgare L . and Their Assessment as an Antimicrobial Agent and Biomedical Application. **2023**.

[42] Jha, S.; Rani, R.; Singh, S. Biogenic Zinc Oxide Nanoparticles and Their Biomedical Applications : A Review. *J. Inorg. Organomet. Polym. Mater.*, **2023**, *33* (6), 1437–1452. https://doi.org/10.1007/s10904-023-02550-x.

[43] Yadav, S.; Shakya, K.; Gupta, A.; Singh, D.; Chandran, A. R.; Varayil, A. A Review on Degradation of Organic Dyes by Using Metal Oxide Semiconductors. *Environ. Sci. Pollut. Res.*, **2023**, *30* (28), 71912–71932. https://doi.org/10.1007/s11356-022-20818-6.

[44] Rambabu, K.; Bharath, G.; Banat, F.; Show, P. L. Green Synthesis of Zinc Oxide Nanoparticles Using Phoenix Dactylifera Waste as Bioreductant for Effective Dye Degradation and Antibacterial Performance in Wastewater Treatment. *J. Hazard. Mater.*, **2021**, *402* (July). https://doi.org/10.1016/j.jhazmat.2020.123560.

[45] Hu, J.; Xianyu, Y. When Nano Meets Plants: A Review on the Interplay between Nanoparticles and Plants. *Nano Today*, **2021**, *38*, 101143. https://doi.org/10.1016/j.nantod.2021.101143.

[46] Dangana, R. S.; George, R. C.; Agboola, F. K.; Samson, R.; George, R. C.; Agboola, F.

K.; Dangana, R. S. Green Chemistry Letters and Reviews The Biosynthesis of Zinc Oxide Nanoparticles Using Aqueous Leaf Extracts of Cnidoscolus Aconitifolius and Their Biological Activities Cnidoscolus Aconitifolius and Their Biological Activities. **2023**. https://doi.org/10.1080/17518253.2023.2169591.

[47] Pradeev raj, K.; Sadaiyandi, K.; Kennedy, A.; Sagadevan, S.; Chowdhury, Z. Z.; Johan, M. R. Bin; Aziz, F. A.; Rafique, R. F.; Thamiz Selvi, R.; Rathina bala, R. Influence of Mg Doping on ZnO Nanoparticles for Enhanced Photocatalytic Evaluation and Antibacterial Analysis. *Nanoscale Res. Lett.*, **2018**, *13*. https://doi.org/10.1186/s11671-018-2643-x.

[48] Mthana, M. S.; Nhlanhla, M.; Ekennia, A. C.; Singh, M.; Onwudiwe, D. C. Cytotoxicity and Antibacterial Effects of Silver Doped Zinc Oxide Nanoparticles Prepared Using Fruit Extract of Capsicum chinense. *Sci. African*, **2022**, *17*, e01365. https://doi.org/10.1016/j.sciaf.2022.e01365.

[49] Abhishek, T.; Sharma, A.; Tejwan, N.; Ghosh, N.; Das, J. A State of Art Review on the Synthesis, Antibacterial, Antioxidant, Antidiabetic, and Tissue Regeneration Activities of Zinc Oxide Nanoparticles. *Adv. Colloid Interface Sci.*, **2021**, *295*, 102495. https://doi.org/10.1016/j.cis.2021.102495.

[50] Neena, D.; Kondamareddy, K. K.; Bin, H.; Lu, D.; Kumar, P.; Dwivedi, R. K.; Pelenovich, V. O.; Zhao, X. Z.; Gao, W.; Fu, D. Enhanced Visible Light Photodegradation Activity of RhB/MB from Aqueous Solution Using Nanosized Novel Fe-Cd Co-Modified ZnO. *Sci. Rep.*, **2018**, *8* (1), 1–12. https://doi.org/10.1038/s41598-018-29025-1.

[51] Bilensoy, E.; Varan, C. Expert Opinion on Drug Discovery Is There a Niche for Zinc Oxide Nanoparticles in Future Drug Discovery ? *Expert Opin. Drug Discov.*, **2023**, *18* (9), 943–946. https://doi.org/10.1080/17460441.2023.2230152.

[52] Sabir, S.; Arshad, M.; Chaudhari, S. K. Zinc Oxide Nanoparticles for Revolutionizing Agriculture : Synthesis and Applications. **2014**, *2014*.

[53] Yi-hao, T.; Hang, Z.; Yin, W.; Ming-hui, D.; Guo, J.; Bin, Z. Facile Fabrication of Nitrogen-Doped Zinc Oxide Nanoparticles with Enhanced Photocatalytic Performance. **2015**, *10*, 432–434. https://doi.org/10.1049/mnl.2015.0130.

[54] Chavillon, B.; Cario, L.; Tessier, F.; Boujtita, M.; Pellegrin, Y.; Blart, E.; Smeigh, A.; Hammarstr, L.; Odobel, F. P-Type Nitrogen-Doped ZnO Nanoparticles Stable under Ambient Conditions. **2012**, 464–470.

[55] Qiu, X.; Burda, C. Chemically Synthesized Nitrogen-Doped Metal Oxide Nanoparticles. *Chem. Phys.*, **2007**, *339* (1–3), 1–10. https://doi.org/10.1016/j.chemphys.2007.06.039.

[56] Gowtham, H. G.; Murali, M. Antioxidant and Photocatalytic Properties of Zinc Oxide Nanoparticles Phyto - Fabricated Using the Aqueous Leaf Extract of Sida acuta. **2022**, 857–867.

[57] Du, W.; Wu, L.; Zhao, J.; Si, W.; Wang, F.; Liu, J.; Liu, W. Engineering the Surface Structure of Porous Indium Oxide Hexagonal Nanotubes with Antimony Trioxide for Highly-Efficient Nitrogen Dioxide Detection at Low Temperature. *Appl. Surf. Sci.*, **2019**, *484* (March), 853–863. https://doi.org/10.1016/j.apsusc.2019.03.329.

[58] Fang, X.; Li, J.; Zhao, D.; Shen, D.; Li, B.; Wang, X. Phosphorus-Doped p-Type ZnO Nanorods and ZnO Nanorod p - n Homojunction LED Fabricated by Hydrothermal Method. **2009**, 21208–21212.

[59] Fan, D.; Zhang, R.; Li, Y. Synthesis and Optical Properties of Phosphorus-Doped ZnO Nanocombs. *Solid State Commun.*, **2010**, *150* (39–40), 1911–1914. https://doi.org/10.1016/j.ssc.2010.07.036.

[60] Mandor, H.; Amin, N. K.; Abdelwahab, O.; Sayed, E.; Ashtoukhy, Z. El. Preparation and Characterization of N - Doped ZnO and N - Doped - TiO 2 Beads for Photocatalytic Degradation of Phenol and Ammonia. *Environ. Sci. Pollut. Res.*, **2022**, *1*, 56845–56862. https://doi.org/10.1007/s11356-022-19421-6.

[61] Muhammad, W.; Ullah, N.; Haroon, M.; Abbasi, B. H. Optical, Morphological and Biological Analysis of Zinc Oxide Nanoparticles (ZnO NPs) Using Papaver. **2019**, 29541–29548. https://doi.org/10.1039/c9ra04424h.

[62] Nur, S.; Mohamad, A.; Shameli, K.; Teow, S.; Chew, J.; Ooi, L.; Soon, M. L.; Ismail, N. A.; Moeini, H. Enhanced Antibacterial and Anticancer Activities of Plant Extract Mediated Green Synthesized Zinc Oxide-Silver Nanoparticles. **2023**, No. July, 1–14. https://doi.org/10.3389/fmicb.2023.1194292.

[63] Prabakaran, E.; Pillay, K. RSC Advances Synthesis of N-Doped ZnO Nanoparticles with Cabbage Morphology as a Catalyst for the e Ffi Cient Photocatalytic Degradation of Methylene Blue under UV and Visible Light. **2019**, 7509–7535. https://doi.org/10.1039/c8ra09962f.

[64] Zhou, X.; Hayat, Z.; Zhang, D.; Li, M.; Hu, S.; Wu, Q.; Cao, Y.; Yuan, Y. Modification,

and Applications in Food and Agriculture. **2023**.

[65] Khamis, M.; Gouda, G. A.; Nagiub, A. M. Biosynthesis Approach of Zinc Oxide Nanoparticles for Aqueous Phosphorous Removal : Physicochemical Properties and Antibacterial Activities. *BMC Chem.*, **2023**, 1–22. https://doi.org/10.1186/s13065-023-01012-2.

[66] Singh, K.; Singh, J.; Rawat, M. Green Synthesis of Zinc Oxide Nanoparticles Using Punica Granatum Leaf Extract and Its Application towards Photocatalytic Degradation of Coomassie Brilliant Blue R - 250 Dye. *SN Appl. Sci.*, **2019**, *1* (6), 1–8. https://doi.org/10.1007/s42452-019-0610-5.

[67] Chen, X.; Wu, Z.; Gao, Z.; Ye, B. C. Effect of Different Activated Carbon as Carrier on the Photocatalytic Activity of Ag-N-ZnO Photocatalyst for Methyl Orange Degradation under Visible Light Irradiation. *Nanomaterials*, **2017**, *7* (9). https://doi.org/10.3390/nano7090258.

[68] Peter, C. N.; Anku, W. W.; Sharma, R.; Joshi, G. M.; Shukla, S. K.; Govender, P. P. N-Doped ZnO/Graphene Oxide: A Photostable Photocatalyst for Improved Mineralization and Photodegradation of Organic Dye under Visible Light. *Ionics (Kiel).*, **2019**, *25* (1), 327–339. https://doi.org/10.1007/s11581-018-2571-x.

[69] Luu, T. V. H.; Luu, M. D.; Dao, N. N.; Le, V. T.; Nguyen, H. T.; Doan, V. D. Immobilization of C/Ce-Codoped ZnO Nanoparticles on Multi-Walled Carbon Nanotubes for Enhancing Their Photocatalytic Activity. *J. Dispers. Sci. Technol.*, **2021**, *42* (9), 1311–1322. https://doi.org/10.1080/01932691.2020.1740728.

[70] Primo, J. D. O.; Bittencourt, C.; Acosta, S.; Sierra-castillo, A. Synthesis of Zinc Oxide Nanoparticles by Ecofriendly Routes : Adsorbent for Copper Removal From Wastewater. **2020**, *8* (November), 1–13. https://doi.org/10.3389/fchem.2020.571790.

[71] Goktas, S.; Goktas, A. A Comparative Study on Recent Progress in Efficient ZnO Based Nanocomposite and Heterojunction Photocatalysts_ A Review. **2021**, *863*. https://doi.org/10.1016/j.jallcom.2021.158734.

[72] Mandor, H.; El-Ashtoukhy, E. S. Z.; Abdelwahab, O.; Amin, N. K.; Kamel, D. A. A Flow-Circulation Reactor for Simultaneous Photocatalytic Degradation of Ammonia and Phenol Using N-Doped ZnO Beads. *Alexandria Eng. J.*, **2022**, *61* (5), 3385–3401. https://doi.org/10.1016/j.aej.2021.08.052.

[73] Helmy, E. T.; Abouellef, E. M.; Soliman, U. A.; Pan, J. H. Novel Green Synthesis of S-Doped TiO2 Nanoparticles Using Malva Parviflora Plant Extract and Their Photocatalytic, Antimicrobial and Antioxidant Activities under Sunlight Illumination. *Chemosphere*, **2021**, *271*, 129524. https://doi.org/10.1016/j.chemosphere.2020.129524.

[74] Bakr, A.; Raghda, M.; Yasmine, M.; Mazen, A.; Rasheed, A.; Abdel, A. M. Zinc Oxide Nanoparticles Promise Anticancer and Antibacterial Activity in Ovarian Cancer. *Pharm. Res.*, **2023**, No. 0123456789. https://doi.org/10.1007/s11095-023-03505-0.

[75] Alaya, L.; Saeedi, A. M.; Alsaigh, A. A.; Almalki, M. H. K.; Alonizan, N. H.; Hjiri, M. ZnO : V Nanoparticles with Enhanced Antimicrobial Activities. **2023**, 1–13.

[76] Jain, D.; Singh, A. Microbial Fabrication of Zinc Oxide Nanoparticles and Evaluation of Their Antimicrobial and Photocatalytic Properties. **2020**, *8* (September), 1–11. https://doi.org/10.3389/fchem.2020.00778.

[77] Ramesh, P.; Saravanan, K.; Manogar, P.; Johnson, J.; Vinoth, E.; Mayakannan, M. Sensing and Bio-Sensing Research Green Synthesis and Characterization of Biocompatible Zinc Oxide Nanoparticles and Evaluation of Its Antibacterial Potential. *Sens. Bio-Sensing Res.*, **2021**, *31* (January), 100399. https://doi.org/10.1016/j.sbsr.2021.100399.